

ML-Based Data-Driven Traffic Flow Estimation from Mobile Data

PEI-LUN HSU

Date: April 27, 2021

Supervisor: Ian Marsh, Xiaoliang Ma

Examiner: Erik Jenelius

School of Electrical Engineering and Computer Science

Host company: RISE SICS AB

Swedish title: ML-baserad datadriven uppskattning av trafikflöden
från mobila data

ML-Based Data-Driven Traffic Flow Estimation from Mobile Data /
ML-baserad datadriven uppskattnig av trafikflöden från mobila
data

© 2021 Pei-Lun Hsu

Abstract

Comprehensive information on traffic flow is essential for vehicular emission monitoring and traffic control. However, such information is not observable everywhere and anytime on the road because of high installation costs and malfunctions of stationary sensors. In order to compensate for stationary sensors' weakness, this thesis analyses an approach for inferring traffic flows from mobile data provided by INRIX, a commercial crowd-sourced traffic dataset with wide spatial coverage and high quality. The idea is to develop [Artificial Neural Network \(ANN\)](#)-based models to automatically extract relations between traffic flow and INRIX measurements, e.g., speed and travel time, from historical data considering temporal and spatial dependencies. We conducted experiments using four weeks of data from INRIX and stationary sensors on two adjacent road segments on the E4 highway in Stockholm. Models are validated via traffic flow estimation based on one week of INRIX data. Compared with the traditional approach that fits the stationary flow-speed relationship based on the multi-regime model, the new approach greatly improves the estimation accuracy. Moreover, the results indicate that the new approach's models have better resistance to the drift of input variables and can decrease the deterioration of estimation accuracy on the road segment without a stationary sensor. Hence, the new approach may be more appropriate for estimating traffic flows on the nearby road segments of a stationary sensor. The approach provides a highly automated means to build models adaptive to datasets and improves estimation and imputation accuracy. It can also easily integrate new data sources to improve the models. Therefore, it is very suitable to be applied to [Intelligent Transport Systems \(ITS\)](#) for traffic monitor and control in the context of the [Internet of Things \(IoT\)](#) and Big Data.

Keywords

Intelligent transport systems, Traffic flow estimation, Machine learning, Artificial neural network, Mobile data, Imputation

Sammanfattning

Omfattande information om trafikflödet är nödvändig för övervakning av fordonsutsläpp och trafikstyrning. Sådan information kan dock inte observeras överallt och när som helst på vägen på grund av höga installationskostnader och funktionsstörningar hos stationära sensorer. För att kompensera för stationära sensorers svagheter analyseras i denna avhandling ett tillvägagångssätt för att härleda trafikflöden från mobila data som tillhandahålls av INRIX, en kommersiell trafikdataset som tillhandahålls av allmänheten och som har en bred rumslig täckning och hög kvalitet. Tanken är att utveckla modeller baserade på artificiellt neuronnät för att automatiskt extrahera relationer mellan trafikflöden och INRIX-mätningar, t.ex. hastighet och restid, från historiska data med hänsyn till tidsmässiga och rumsliga beroenden. Vi utförde experiment med fyra veckors data från INRIX och stationära sensorer på två intilliggande vägsegment på E4:an i Stockholm. Modellerna valideras via uppskattning av trafikflödet baserat på en veckas INRIX-data. Jämfört med det traditionella tillvägagångssättet som anpassar det stationära sambandet mellan flöde och hastighet baserat på multiregimmodellen, förbättrar det nya tillvägagångssättet noggrannheten avsevärt. Dessutom visar resultaten att modellerna i den nya metoden är bättre motståndskraftiga mot avvikelser i ingående variabler och kan minska försämringen av noggrannheten på vägsegmentet utan stationär sensor. Den nya metoden kan därför vara lämpligare för att uppskatta trafikflöden på de närliggande vägsegmenten med en stationär sensor. Metoden ger ett mycket automatiserat sätt att bygga modeller som är anpassade till datamängder och förbättrar noggrannheten vid uppskattning och imputering av trafikflöden. Den kan också enkelt integrera nya datakällor för att förbättra modellerna. Den är därför mycket lämplig att tillämpa på intelligenta transportsystem för trafikövervakning och trafikstyrning i samband med sakernas internet och big data.

Nyckelord

Intelligenta transportsystem, Uppskattning av trafikflödet, Maskininlärning, Artificiellt neuronnät, Mobila data, Imputering

Contents

1	Introduction	1
1.1	Background	2
1.2	Problem	2
1.3	Goal and Purposes	3
1.4	Contributions	4
1.5	Research Methodology and Ethics	5
1.6	Delimitations	5
1.7	Structure of the thesis	6
2	Background	7
2.1	Traffic State Variables	7
2.2	Sensor Data Types	8
2.3	Traffic State Estimation and Imputation	9
2.4	Traffic State Estimation Approaches	11
2.5	Fundamental Diagrams	12
2.6	Machine Learning Methods	14
2.6.1	Linear Regression	14
2.6.2	Polynomial Regression	16
2.6.3	Artificial Neural Network	17
3	Related Work	20
4	Datasets and Methodology	24
4.1	Datasets	24
4.1.1	INRIX	25
4.1.2	Motorway Control System (MCS)	27
4.2	Data Preparation	28
4.3	Models	30
4.3.1	Baseline Model	30
4.3.2	Neural Network Models	31

4.4	Performance Evaluation	35
5	Results	37
5.1	Data Preparation Results	37
5.2	Model Training Results	40
5.3	Traffic Flow Estimations	44
6	Discussion	51
6.1	Input Speed Drift	51
6.2	Travel Time	54
6.3	Spatial Dependency	57
6.4	Model Usage and updates	59
7	Conclusion and Future work	62
7.1	Future work	63
7.1.1	Spatial-Temporal Correlations	63
7.1.2	Traffic Flow Prediction	64
7.1.3	Others	64
	References	67

List of Figures

2.1	Relation of traffic data and traffic state in the space-time domain. Adapted from [2].	10
2.2	Flow-speed and flow-density FD.	13
2.3	Dataset with linear relationship and linear regression model predictions.	15
2.4	Architecture of a neural network with one input layer, one hidden layer, and one output layer. Adapted from [30].	17
4.1	Locations of INRIX segments and MCS sensors in Stockholm.	25
4.2	Structure of the neural network considering temporal dependencies.	32
5.1	Time-series INRIX speed and MCS flow before and after smoothing on 1 st October.	38
5.2	INRIX and MCS speed versus time (epoch) before and after shifting INRIX timestamps on 1 st October.	39
5.3	Distributions of INRIX speed in training and test datasets before and after the standardization.	40
5.4	Baseline versus univariate ANN flow-speed relationship.	41
5.5	Training samples' different flow-speed behaviors in different time segments.	42
5.6	Temporal ANN model considering flow-speed relationship's dependencies to the hour of a day and the day of a week.	43
5.7	Overview of the flow estimation performance on the two consecutive road segments.	44
5.8	Examples of estimated flows using temporal ANN (speed, travel time) on the south segment.	48
5.9	Examples of estimated flows using temporal ANN (speed, travel time) on the north segment.	49

6.1	Distributions of input speed in the training and test datasets before and after the standardization for the ANN (speed) model.	52
6.2	Test samples from both road segments and corresponding flow estimations given by the baseline model.	53
6.3	Test samples from both road segments and the corresponding flow estimations given by the ANN (speed) model.	54
6.4	Relationship between speed and travel time in the training dataset from the south road segment.	55
6.5	Distributions of travel time in the test datasets before and after the standardization.	56
6.6	Spatiotemporal ANN's flow estimations on both road segments.	57
6.7	Conceptual representation for a road segment between two fixed sensors with a speed limit transition.	60

List of Tables

4.1	INRIX ID and MCS ID for corresponding road segments.	24
4.2	The schema and example of the INRIX dataset	26
4.3	The schema and example of the MCS dataset	27
4.4	Example of one-hot encoding features for temporal and spatial factors.	29
5.1	Training errors for baseline and univariate ANN flow-speed relationship model.	40
5.2	Improvements of flow estimation performance in MAPE achieved by ANN models over the baseline model.	46
5.3	Improvements of flow estimation performance in RMSE achieved by ANN models over the baseline model.	46

List of acronyms and abbreviations

AI Artificial intelligence

ANN Artificial Neural Network

ARIMA Autoregressive Integrated Moving Average

AVI Automatic Vehicle Identification

CNN Convolution Neural Network

CSV Comma-Separated Value

FD Fundamental Diagram

GCN Graph Convolutional Network

GDPR General Data Protection Regulation

GPS Global Positioning System

ICT Information and Communication Technology

IoT Internet of Things

ITS Intelligent Transport Systems

KNN K-Nearest-Neighbor

LSTM Long Short-Term Memory

MAPE Mean Absolute Percentage Error

MCS Motorway Control System

ML Machine Learning

MLP Multi-Layer Perceptron

MSE Mean Squared Error

RMSE Root Mean Square Error

RNN Recurrent Neural Network

TSE Traffic State Estimation

Chapter 1

Introduction

Rapid urbanization and the growing need for traveling have resulted in several traffic-related challenges in urban road networks. As one of the main challenges, traffic congestion results in extra travel time and fuel consumption and increases vehicular emission, which is related to air pollution and climate change [1, 2]. Therefore, it is crucial for road authorities to implement effective traffic control measures, such as ramp metering and variable speed limits, to effectively mitigate congestion and its negative effects, e.g., high vehicular emission [2, 3]. To implement efficient traffic control measures and monitor vehicular emission on the roads, accurate traffic state information with a high spatiotemporal resolution is necessary [2, 3].

Unfortunately, traffic variables such as flow and density that characterizing the traffic state are not observable everywhere on roads because of the high installation and maintenance costs of traditional stationary sensors. Moreover, most of the traffic datasets collected from stationary sensors have missing data due to sensor malfunctions and communication failures [4]. Therefore, we need to estimate the traffic state variables in the unobserved regions or impute the missing traffic data based on partially observed traffic data to provide accurate traffic monitoring and control [2]. In the past decades, new traffic data sources such as smartphones and on-vehicle navigation systems have emerged because of the advances in **Information and Communication Technology (ICT)** and the recent trend of the **IoT**. The mobile data, also known as probe vehicle data, collected from these new data sources have broader coverage of road networks than the stationary sensor data, hence providing additional traffic information for **Traffic State Estimation (TSE)**. Many researchers have been investigating how to use mobile data for estimating the traffic state variables [5, 6, 7, 8]. ITSs are systems that apply **ICT**, e.g., **Artificial intelligence (AI)**,

in the field of road transportation and traffic management [9, 10]. Three essential components are necessary for an ITS function: data collection, data analysis, and data/information transmission [10]. The traffic estimation approach proposed in this work can be regarded as a part of ITS’s data analysis component, which automatically builds models for estimating or imputing traffic flow on highways using mobile data. The ANN models generated by the approach can produce more accurate results than the classic multi-regime regression model by better modeling the time- and space-varying relationships between traffic flow and speed. Moreover, the approach is flexible to integrate multiple available information sources. It can be easily implemented into a pipeline application that automates estimator building processes for ITS via any common data processing and deep learning libraries, e.g., TensorFlow.

The approach proposed in this work is trained and tested using both stationary and mobile datasets collected on road segments in Stockholm’s high system during October 2018.

1.1 Background

The thesis project is a part of the TENS project, an ongoing research project at RISE, the Research Institutes of Sweden, SICS. All the datasets for this work were used with RISE permission for research purposes in the TENS-project¹. The TENS project’s goal is network-wide monitoring of road traffic-induced energy consumption and vehicular emission based on alternative traffic data sources. To precisely calculate the vehicular emission and energy consumption, comprehensive information of traffic state variables, i.e., speed and flow, in a road network’s spatiotemporal domain is necessary.

1.2 Problem

As mentioned in the previous sections, the thesis project aims to develop an automated approach for estimating or imputing traffic flow using new traffic sensor data, i.e., mobile data, to provide traffic state information on highways with a high spatiotemporal resolution. Although researchers have proposed various approaches, many of them modeled the stationary relationships between flow and a traffic variable, e.g., speed, then used these relationships to estimate the traffic flow based on traffic measures from mobile

¹ www.tens-project.info

data. One problem with these classic approaches is that traffic relationships are dynamic, which may vary depending on many factors, e.g., time and space. Failed to consider these factors may lead to estimation results with low accuracy. Moreover, those approaches usually require manual efforts by human experts, e.g., mathematical form selection, parameter calibration, and traffic regime identification, to build the estimation models, which means they are not automatic and will not be scalable solutions for flow estimation in networks with a large number of road segments and sensors. Finally, the existing TSE approaches cannot incorporate multiple data sources and capture the complex relationships between them to improve the accuracy effectively. On the other hand, very few studies utilize alternative sensor data to impute the missing or corrupted traffic data among studies in traffic imputation. Therefore, some main questions posed in this thesis project are:

1. Is it possible to develop a flow estimation model with improved accuracy by better modeling the relationship between flow and speed from probe vehicles? Can we improve the accuracy by considering the temporal and spatial dependencies in the relationship?
2. Is it possible to implement a highly automated approach that builds the models automatically and regularly for traffic flow estimation in highway networks?
3. Can we develop an approach that allows for easy incorporation of additional information from available data sources into traffic flow estimation and imputation? Will the additional information help improve the estimation accuracy?

1.3 Goal and Purposes

The thesis's goal is to develop an automated approach for estimating or imputing the traffic flow on a highway with high spatiotemporal resolution using mobile data accurately and efficiently. The approach could be used to build an intelligent transportation system capable of network-wide traffic and emission monitoring. ANN is a data-driven Machine Learning (ML) method that is powerful to learn highly nonlinear relationships in high-dimensional data [11], which is believed to be suitable for modeling complex relationships lying in transportation datasets [12]. Therefore, the project's primary purpose is to explore the potentials of ANNs, a data-driven technique, for traffic flow estimation and evaluate their accuracy, i.e., estimation error, by comparing

them with the classic multi-regime regression model. More specifically, the thesis project implements various ANN-based flow estimation models and evaluating their performance on the training highway segment and its neighboring road segment for the following minor purposes:

1. Implement a uni-variate model to answer whether ANN can better model the stationary traffic flow relationship than the classic multi-regime model.
2. Implement multivariate ANN models to answer whether incorporating an additional traffic variable from mobile data, e.g., travel time, could help improve the estimation accuracy.
3. Implement time-dependent models to answer whether ANN can capture time-varying traffic flow relationships.
4. Implement a time-space-dependent model to answer whether ANN can capture the spatiotemporal dependency of the traffic flow relationships lying in the datasets with sensor data from multiple road segments.

1.4 Contributions

The thesis's main contributions to the research area of traffic flow estimation, imputation, and intelligent transportation systems are as follows:

1. Propose an approach for traffic flow estimation from mobile data that significantly improve the accuracy of estimation by using ANN, a data-driven technique, compared to the traditional multi-regime model. Evaluate the estimation error for ANN models using mobile data in the unobserved area and time periods.
2. Evaluate and demonstrate ANNs' ability to model time-dependent flow-speed relationship and their ability to incorporate multiple data sources into the estimation flexibly.
3. Implement the estimation approach in an open-source application¹ using Python, pandas, and the ML libraries scikit-learn and TensorFlow. The application can automatically and regularly build flow estimation models for road segments with different traffic characteristics in a road network without the need for human intervention.

¹ <https://github.com/plhsu19/traffic-flow-esimation>

4. Show the possibility of reducing the number of models needed to estimate traffic flow on the road or in a road network by training a more efficient central ANN model that can capture the network-wise spatial and temporal dependencies for the entire road/network.
5. Show the possibility of incorporating alternative data sources into imputing missing data instead of only using spatial and temporal information in the datasets like most recent imputation studies.

1.5 Research Methodology and Ethics

This thesis project adopted a mixture of quantitative and qualitative research methods, i.e., triangulation research method [13]. As we aim to develop ANN-based traffic estimation models using training datasets and validate the models on test datasets by numerical metrics, it satisfies the description of Quantitative Research Method, which according to Håkansson is “The method requires large datasets and use statistics to test the hypothesis and make the research project valid” [13]. On the other hand, we performed the explorative analysis to understand the characteristics of variables/features in traffic datasets and use them to improve our ANN models, which belongs to the Qualitative Research method.

Regarding ethical issues, data collection from the smartphones, Global Positioning System (GPS) devices, and other mobile sensors should comfort the General Data Protection Regulation (GDPR) as they are a kind of private data. Also, there should not be any negative effect on sustainability or social issues come from this thesis project.

1.6 Delimitations

The project has the following limitations because of the nature of data sources and the purpose of the project:

1. The proposed approach is an off-line one designed for building models to estimate or impute traffic flow using batch datasets rather than using streaming data. However, it is possible to implement the approach in Apache Spark Streaming or Apache Flink for streaming processing and real-time estimation/imputation.
2. The proposed models cannot forecast future traffic conditions based on the observed traffic sensor data. It is developed to estimate the traffic

flow in the unobserved region or impute the missing data in the traffic flow datasets using partially observed traffic data, i.e., mobile data. However, predicting the future traffic flow using various data sources could be a topic for future research.

3. Although we incorporate the temporal factor, i.e., weekday and hour, and spatial factor, i.e., location, as input features to capture the time-space-varying traffic flow conditions, we do not actually use the temporal and spatial correlations between subject data point and its neighboring data points for estimation/imputation. Again, mining the spatial and temporal information in the alternative sensor datasets and utilizing them for traffic estimation/imputation/prediction will be a possible future work.

1.7 Structure of the thesis

The rest of the thesis is organized as follows: Chapter 2 presents the thesis project's background, including fundamental knowledge of TSE, and the machine learning methods used in this work. Chapter 3 presents the related work in data-driven TSE using probe vehicle data as well as works in traffic data imputation. Chapter 4 deals with the datasets and methods used to implement the traffic flow estimation approach, including the introduction of datasets, data preparation, model structures, and performance evaluation. Chapter 5 details the results of the implementation and the evaluation of estimation models. We also analyze and discuss the results in chapter 6. Chapter 7 gives the conclusion of the thesis as well as some suggestions for future works.

Chapter 2

Background

This chapter provides users with background knowledge about the traffic state estimation in ITS, including traffic state variables, sensor data types, traffic state estimation/imputation, TSE approaches, fundamental diagrams, and adopted machine learning methods, which are necessary for readers to understand this work. The chapter is composed of six sections corresponding to each topic listed above.

2.1 Traffic State Variables

This section aims to provide necessary information about the fundamental traffic state variables that are widely used to assess the traffic state. From a macroscopic view, the state of traffic on highways can be represented by three fundamental variables, speed, flow, and density [2, 14]. We often assess the traffic on highways by describing the movement of a group of vehicles as a stream flowing through the road segment at a macroscopic scale, rather than describing each vehicle's movement at a microscopic scale [14]. These three variables are therefore used to describe the traffic flow on highway segments. The definitions of the three variables are as follow:

Flow is defined as the number of vehicles travel through a particular point or highway segment per unit of time [14]. It is typically expressed in vehicles per hour (veh/h) [2, 14].

Speed is measured in units of distance per unit of time. It is typically expressed in miles per hour (mph) [14], kilometers per hour (km/h) [2], or meters per second (m/s). Average speeds are often used to describe the movement of the traffic flow [2, 14]. There are two ways to obtain average speeds, one is time-mean speed, and another is space-mean speed [14]. For

the time-mean speed, instantaneous speeds of all vehicles passing through a particular location are measured, and the average speed is calculated from those instantaneous speeds at that location. For the space-mean speed, the travel time of each vehicle between two particular locations is measured, and the average speed is calculated by dividing the distance between two locations by the average travel time.

Density is defined as the number of vehicles per unit of distance, which is typically expressed as vehicles per mile (vpm) [14], or vehicles per kilometer (veh/km) [2]. In traffic flow models, the relationship of three variables satisfies the equation [2, 14]:

$$\text{Flow} = \text{Speed} \times \text{Density} \quad (2.1)$$

Therefore, one can estimate the third variable when any two of variables are known [14].

We are primarily interested in traffic flow and speed in this work without including density into our estimation models for two reasons. First, density is difficult to measure directly with the current sensor technology [14]. The two sensor systems that we use also do not provide the measurement of density. Second, a subset of three variables, e.g., flow-speed, is typically sufficient to represent the traffic state because the remaining variable can be estimated using equation 2.1. In our case, knowing the flow and speed as well as their relationship is sufficient for our use case, which aims to monitor the traffic states in the road network system using alternative data sources, and based on which calculates the energy consumption.

2.2 Sensor Data Types

The traffic measurement data, which can provide us with information on microscopic traffic state variables and other traffic characteristics, can be grouped into two categories based on the ways they are collected: stationary data and mobile data.

Stationary data is collected by stationary sensors installed on highways, e.g., inductive loop, ultrasonic detector, and radar detector [2]. These stationary sensors collect vehicle data at the installed locations, which is the conventional way to assess highway traffic adopted by road authorities. Stationary data can provide macroscopic variable flow and average speed based on the direct measurement of vehicle count and the instantaneous speed of individual vehicles passing the sensor locations. Although a full subset of traffic state

variables can be obtained from the stationary data, the stationary sensors are only installed sparsely on highways, usually with the inter-sensor space ranging from hundred meters to several kilometers, because of the high installation and maintenance costs [2]. Therefore, the stationary data's spatial regions are limited to the specific locations where the sensors are installed. Moreover, stationary sensors suffer from reliability problems such as missing counts, which results in missing data and invalid data [4, 15].

Mobile data is collected by on-vehicle sensor systems, e.g., GPS and Automatic Vehicle Identification (AVI) [2, 3, 16], which have been widely adopted in recent years because of advances in the ICT. Vehicles with these on-vehicle sensors such as GPS in the navigation systems and RFID installed in license plates are usually referred to as the probe vehicles. On-vehicle sensors can measure probe vehicles' trajectories, which is the microscopic information describing each vehicle's behavior. Trajectory information from mobile data can also be aggregated to obtain the average speed and other traffic performance measures with a specific spatiotemporal resolution [2, 17]. Mobile data typically can cover a spatial border region than stationary data because on-vehicle sensors are not confined in fixed locations like stationary sensors. However, it is challenging to estimate the flow and density solely based on mobile data without additional data sources because of the low penetration rate of probe vehicles [3]. Therefore, it is usually impossible to obtain a full subset of the traffic state variables, e.g., flow-speed or density-speed, from the mobile data.

The same type of traffic variable/data provided by different sensor systems could be different. For example, the average speed reported by INRIX, one of the major mobile data providers, is widely found to exhibit a bias and latency relative to the average speed reported by stationary sensors, e.g., loop detectors, at the same road segment because of reasons such as measurement techniques and speed calculation [17, 18]. Therefore, we should be careful about these differences when incorporating traffic data from various data sources into an estimation model or ITS.

2.3 Traffic State Estimation and Imputation

According to Seo et al. [2], “*Traffic State Estimation refers to the process of inference of traffic state variables, namely flow (veh/h), density (veh/km), speed (km/h), and other equivalent variables, on road segments, using partially observed and noisy traffic data.*” As we mentioned in the introduction, accurate information of traffic state is essential for traffic control [2], traffic

emission monitoring [3], and the development of ITS [19]. However, traffic state variables are not observable everywhere and anytime on highway segments. We need to estimate the traffic state in the regions where traffic state variables are not observed or partially observed.

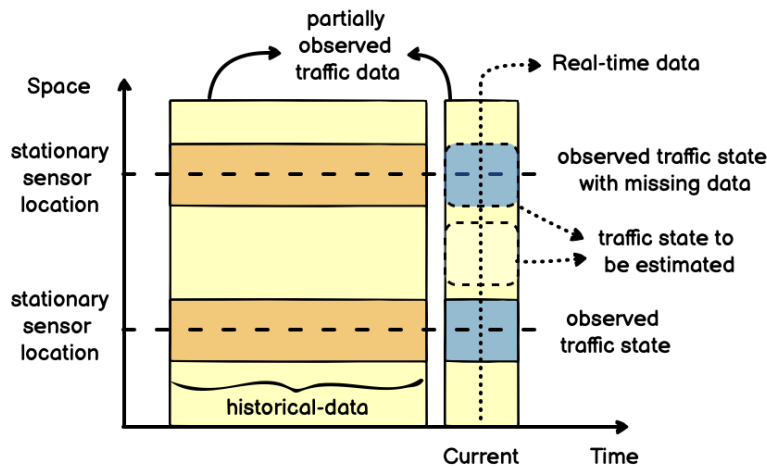


Figure 2.1 – Relation of traffic data and traffic state in the space-time domain. Adapted from [2].

Figure 2.1 is a conceptual diagram adapted from [2], which describes the traffic data, traffic state, and their relation in the time-space domain. As mentioned before, a subset of traffic state variables can represent a traffic state on highways, i.e., any two of three traffic state variables [2]. In figure 2.1, the traffic state is observable at the locations where stationary sensors are installed. However, stationary sensors are usually installed sparsely on highways due to cost reasons. In the regions outside stationary sensors' coverage, the yellow regions in figure 2.1, traffic state variables are either unobserved or only partially observed through traffic data collected by other sensors, e.g., mobile devices. TSE aims to estimate the unobserved traffic state variables using partially observed traffic data in regions where stationary sensors are absent, e.g., the yellow region with the dashed boundary in figure 2.1. Moreover, even at the locations where stationary sensors are installed, traffic datasets usually suffer from missing or corrupted data due to failures of sensors or communication [4, 15]. Therefore, a specific TSE method called imputation has been developed for imputing the missing or corrupted data in the traffic datasets collected from the locations where the sensors are installed but suffer from missing data.

Data in figure 2.1 can be categorized into two groups according to the

time when they are collected. If the data is collected when the traffic state is estimated, it is called real-time data or streaming data [2]. Real-time data includes all traffic data collected by various sensors from the estimation location and its neighboring locations. On the other hand, if the traffic data is collected for a long time before the moment of estimation, it is called historical data, which also includes various types of traffic data collected from locations of interest. All TSE and imputation methods use real-time data and models to infer traffic state variables, but not every one of them needs historical data. Historical data is utilized to develop models and train them by some TSE approaches.

Various TSE approaches, e.g., model-driven, data-driven, and streaming-data-driven approaches, are used for inferring traffic state variables in the time-space regions of interest, which will be introduced in the next section. From now on, "time-space region/domain" and "spatiotemporal region/domain" will be used interchangeably.

2.4 Traffic State Estimation Approaches

According to the classifying method proposed by Seo et al. [2], TSE approaches can be grouped into three categories, i.e., model-driven, data-driven, and streaming-data-driven, depending on whether the approach needs a pre-determined assumption, i.e., a traffic flow model, and the data type they used. The approach adopted by this work belongs to the data-driven approach.

The **model-driven approach** uses pre-determined physical traffic flow models to estimate the traffic state [2]. Those traffic flow models describing the dynamic of traffic were developed based on physical principles and empirical relations. They are well-formulated with a fixed model structure, e.g., functional forms, and a fixed number of parameters. The model parameters, i.e., the functions' parameters, are calibrated by historical data collected on the road segments/networks where the models will be implemented. The calibrated model will then estimate the traffic state in an unobserved region using real-time data as input. The model-driven approach is the most popular type of TSE approach that has been adopted by various studies in TSE, which could estimate traffic states accurately under ordinary traffic conditions [2].

The **data-driven approach** relies solely on historical data collected on the road without using physical models [2]. It extracts the relationships between multivariate traffic variables from historical data, e.g., the dependence between the traffic state variable to be estimated and other observed variables, using statistical or ML methods. Similar to the model-driven approach, the

data-driven approach uses the extracted dependence model to estimate the current traffic state based on real-time data. The same type of approach is also referred to as the "non-parametric approach" in the field of AI and traffic prediction [20], where machine learning models are extensively used. Non-parametric means both of the model structure, e.g., statistics functional form or ML algorithms, and the model parameters, i.e., functions' parameters or algorithms' parameters, are not determined in advanced but determined from the traffic data based on some evaluation metrics, e.g., RMSE and MAPE [20]. Typically, a large amount of historical data is needed by data-driven approaches for building the dependence model. Recent ICT advances, e.g., IoT, have generated data increasingly from different sensor sources that are available for developing various data-driven approaches. Data-driven approaches, especially nonlinear ones such as neural networks, are good at modeling complex nonlinear relationships and traffic dynamics in the transportation field [2, 12, 20]. Moreover, it does not need or need less prior knowledge on traffic to estimate the traffic state [3]. Generally speaking, the data-driven approach needs less domain-specific knowledge of the traffic process for estimation.

The **streaming-data-driven approach** uses only real-time data, i.e., streaming data, and some weak assumptions to estimate the traffic state in the unobserved region [2]. Weak assumptions are some basic principles, e.g., conservation law in traffic flow theory, supported by physical theory and does not need empirical justification [2]. Streaming-data-driven approaches do not need to extract dependence from historical data like data-driven approaches or calibrate the model parameters using historical data like model-driven approaches. However, it needs a large amount of streaming data to estimate the traffic state and usually has lower estimation accuracy than data-driven and model-driven approaches. On the other hand, because it does not rely on any empirical relations, it is more robust under uncertain phenomena and unpredictable conditions, e.g., traffic accidents [2].

2.5 Fundamental Diagrams

Fundamental Diagram (FD) are diagrams used in traffic flow theory to describe relations between traffic flow variables, i.e., flow, density, and speed, for a stationary traffic flow, where all vehicles have the same speed and spacing [10, 21]. Three diagrams in use are flow-density, flow-speed, and speed-density diagrams.

FD contains essential information on traffic characteristics such as free-

flow speed, flow capacity, jam density, and the distinction between different traffic regimes, e.g., congested and free-flow regimes, essential for traffic control and traffic simulation [22, 23]. Because FD describes the relations between traffic state variables, it is also utilized by both model-driven TSE [23] and data-driven TSE [5] to estimate unobserved traffic state variables based on observed variables. Various mathematical functions have been proposed to describe empirical relations between traffic state variables in FDs using curve fitting techniques or traffic theories [2, 21]. Figure 2.2 is an example of FD based on the popular triangular model proposed by Newell [24].

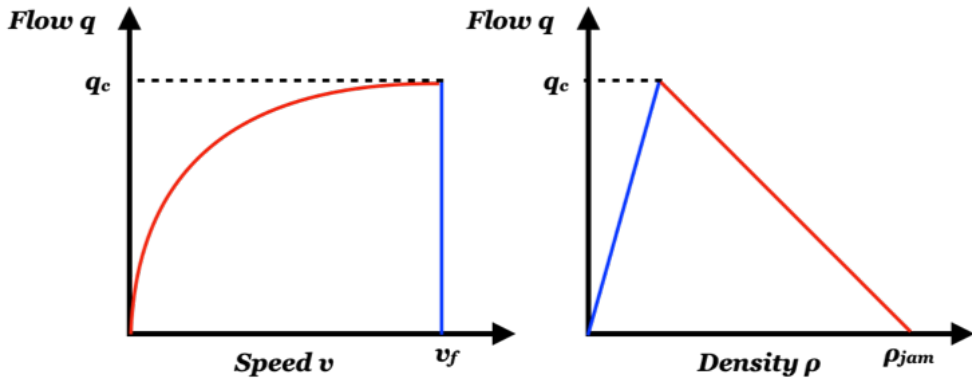


Figure 2.2 – Flow-speed and flow-density FD.

In figure 2.2, every point on the curve of the flow-speed relationship represents a specific traffic state characterized by flow and average speed. The density could be calculated based on flow and speed using equation 2.1. Some traffic state points in the FD provide us with essential information about highway facility traffic features. For the rightmost part of the flow-speed relation curve, i.e., the blue line, vehicles can travel at the maximum speed without inference from other vehicles in the traffic flow. The maximum speed is called free-flow velocity v_f , which depends on the operation's speed restrictions at a particular time and weather [25]. This traffic condition is called a free-flow regime, within which the density of vehicles is generally low. In the free-flow regime, the flow rate value can vary widely while the velocity remains constant. The maximum flow rate q_c in the FD represents the road's capacity [25]. As the speed drops below v_f , the congestion begins, and the flow rate starts to decrease. The red curves in figure 2.2 represent the congested regime, where the speed and flow decrease while density increases. When the traffic is severely congested, flow and speed approach zero, and all vehicles are standstill. This traffic state is usually called traffic jam, and the

density in this state is called jam density, ρ_{jam} .

Although the FDs were assumed to be invariant, the relation between traffic state variables in the real-world is not invariant but dynamic. The parameters of the relationship function and the function itself, i.e., the mathematical formula, vary depending on various factors. For example, many studies found that the empirical flow-speed relation observed at the same road segment varies on different days and in different traffic conditions [6, 22, 26]. The shapes of FD diagrams at different road segments collected from the same area could also be very different [7]. Factors such as time, weather, road surface, accident, driver characteristics, and vehicles' composition can affect the shape of FDs [2, 21].

Many recent studies tried to capture the dynamic FD-relations using methods such as dynamically calibrating the model parameters or using ML clustering techniques to extract the relations [6, 26, 27]. The baseline model in this work is like a conventional static FDs used in many TSE studies [5, 7, 28], whose flow-speed relation does not change with time, space, and other factors. On the other hand, the ANN model proposed is more like a dynamic FD, which considers multiple factors, e.g., time, space, and other available features, that may affect traffic variables' relations.

2.6 Machine Learning Methods

This section aims to introduce machine learning methods utilized in this work for extracting dynamic relations between traffic variables to empower our traffic flow estimator. Section 2.6.1 and 2.6.2 introduce two simple machine learning models, linear regression and polynomial regression, which are used in our baseline model. Section 2.6.3 introduces the deep neural network, an advanced machine learning method also known as deep learning. It is the main method used in this work to build the estimation model.

2.6.1 Linear Regression

Linear regression is one of the simplest machine learning techniques that have been widely used in both academic studies and industrial applications. Linear regression is a linear approach to model the relationship between a dependent variable, i.e., the value to predict, and independent variables, i.e., the feature values [29, 30]. It assumes that the dependent variable is a linear combination of the parameters and the independent variables.

A typical linear regression model predicting a dependent variable based on multiple input features can be expressed as equation 2.2 [30]:

$$\hat{y} = w_0x_0 + w_1x_1 + w_2x_2 + \cdots + w_nx_n \quad (2.2)$$

In equation 2.2, \hat{y} is the predicted value, n is the number of features, and x_i is the i^{th} feature value. w_j is the j^{th} model parameter, which is the feature weight determining how much the j^{th} feature affects the prediction. w_0 represents the bias term, i.e., intercept, while x_0 is always set to 1. Figure 2.3 shows a training dataset and the predictions from a linear regression model with one dependent variable x_1 . To be noticed that, it is typical to call the action of inferring dependent variables from features "prediction" in ML field. Therefore, we use "predict/prediction" instead of "estimate/estimation" in this section to conform with the tradition.

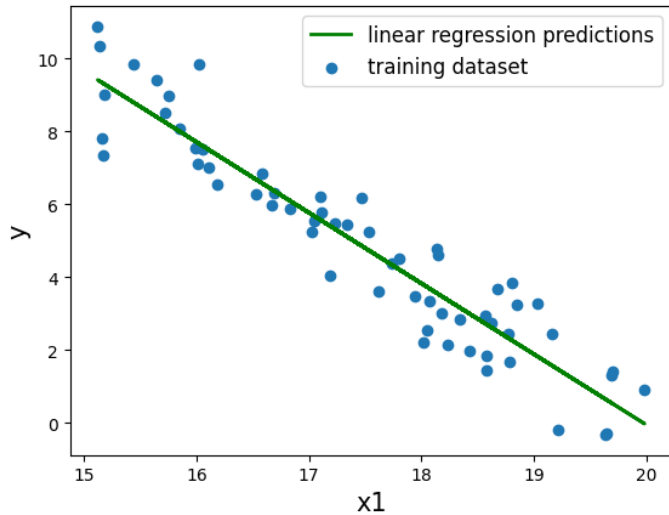


Figure 2.3 – Dataset with linear relationship and linear regression model predictions.

One crucial question is, how do we find the model parameters that best fit the training dataset? To solve the problem, we first need to define a cost function to measure the difference between the model's predictions and the training examples. The most popular cost function used for the linear regression model is Mean Squared Error (MSE), which is shown as equation 2.3 [30]:

$$J(\mathbf{w}) = MSE(\mathbf{w}) = \frac{1}{m} \sum_i^m (\hat{y}^i - y^i)^2 \quad (2.3)$$

In equation 2.3, w is the parameter vector, and m is the number of samples in the training dataset. y^i is the dependent variable's value of i^{th} sample, while \hat{y}^i is the corresponding predicted value by the linear regression model. $J(w)$ is defined as the MSE of the model, which measures how close the predicted values to the real values under a particular value of w . The goal of learning is to choose model parameters that minimize the cost function so that the prediction values are closest to the values in the training dataset.

Two popular approaches are utilized by machine learning software frameworks to find model parameters, the Normal Equation and the Gradient Descent [30]. For the first approach, one directly solves the normal equation, where the gradient of cost function equals 0, to obtain the parameter vector w that minimizes the cost function [30]. However, the computational complexity for solving the normal equation is $O(n^3)$, which make this approach very slow while the number of features in equation 2.2 grows large. Another approach is gradient descent, which finds the optimal solution of model parameters that minimize the cost function by changing the parameters iteratively [30]. The algorithm of gradient descent starts from a parameter vector w with random values, then iteratively changes the parameters toward the direction of the descending gradient until the cost function converges to the minimum value. This optimization algorithm is more computationally efficient than solving the normal equation when the number of features is large. Gradient descent not only can be used to find the optimal solution for linear regression, but it is also the core algorithm for training neural networks, which will be introduced in section 2.6.3.

Many TSE and traffic forecasting studies used linear regression as their prediction model or as a baseline model to compare with more sophisticated models [7, 15, 31]. Its simplicity and computational efficiency give it a competitive edge while memory constraint and short execution time, e.g., real-time application, are critical requirements.

2.6.2 Polynomial Regression

Polynomial regression is a technique that uses the linear model to fit the nonlinear relationships [30]. It adds the power of the independent variables x in equation 2.2 as new features to model the nonlinear relationship between x and the predicted value \hat{y} . For example, a univariate nth degree polynomial regression model can be expressed as equation 2.4:

$$\hat{y} = w_0x_0 + w_1x + w_2x^2 + w_3x^3 + \cdots + w_nx^n \quad (2.4)$$

Although one could use polynomial regression to fit nonlinear relationships between variables, polynomial regression is considered to be a kind of linear regression since the predicted value is still a linear combination of parameters and independent variables. One should avoid overfitting when using high-degree polynomial regression to fit the data by using techniques such as cross-validation. Some studies of FD used polynomial regression as the model to fit the nonlinear relationships between traffic state variables [26].

2.6.3 Artificial Neural Network

The artificial neural network, or just the neural network, is originally a computational model inspired by the biological neural networks proposed by McCulloch [32]. As the subject evolved, many improvements in model structures, e.g., Multi-Layer Perceptron (MLP) [33], and algorithms for training multi-layer neural networks, e.g., backpropagation algorithm, were proposed [34], which form the deep neural networks we are using nowadays. Following the increasing computational power because of the exponential increment of transistor number in microprocessors, more practical neural networks can be deployed by the computers after the 1980s.

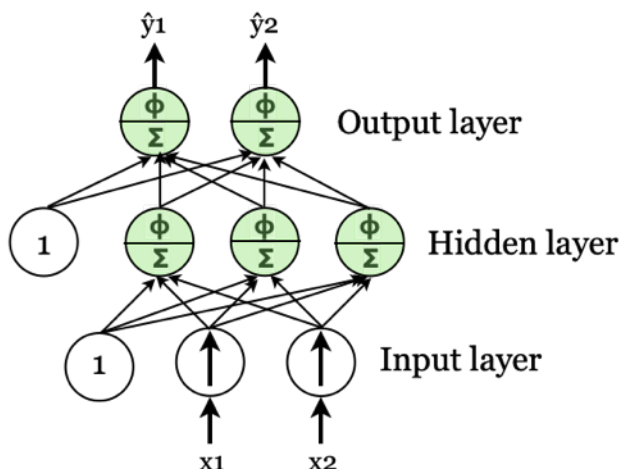


Figure 2.4 – Architecture of a neural network with one input layer, one hidden layer, and one output layer. Adapted from [30].

Figure 2.4 shows the architecture of a neural network with one input layer, one hidden layer, and one output layer. The structure is also called MLP or deep neural network because it has more than one layer of perceptron in the model. The input layer includes the input feature variables of the model

plus a bias input which always equals one. Each green node in the figure is an artificial neuron, which emulates the biological neuron. Each neuron has several input neurons as well as a bias input. Each input connection has its corresponding weight. The neuron computes the weighted sum of all inputs, then apply an activation function to the weighted sum, whose output value will be the output of the neuron. There is a wide range of choices for the activation function, e.g., sigmoid, tanh, and ReLu [30], which should be chosen carefully considering functions' performance and the type of prediction problem to solve. The outputs of neurons in a layer will be the input for neurons in the next layer. The last layer's outputs, i.e., the outputs of the output layer, are the predicted values of the whole neural network. As the signal can only flow in one direction from the input layer, through hidden layers, to the output layer, this architecture is also called feed-forward neural network. The outputs of a whole neuron layer can be computed with equation 2.5 [30]:

$$h_{\mathbf{W}, \mathbf{b}}(\mathbf{X}) = \phi(\mathbf{X}\mathbf{W} + \mathbf{b}) \quad (2.5)$$

In equation 2.5, \mathbf{X} is the matrix of input features or input neurons. Each row represents an instance, and each column represents an input feature/neuron. \mathbf{W} is the weight matrix contains all connection weights for inputs except the weights for the bias input. \mathbf{b} is the bias vector contains the weights for the bias input, which has one weight value for each neuron in the layer. \mathbf{W} and \mathbf{b} are model parameters of the neural network, which should be initialized randomly and learned from the training data. ϕ represents the activation function of the neurons. For hidden layers, it is usually a nonlinear function in order to add nonlinearity to the neural networks. For output layers, the choice of activation function dependents on the type of prediction problem, e.g., sigmoid is usually used for binomial classification. In contrast, a simple linear function is used for regression problems.

To learn neural network's model parameters, i.e., \mathbf{W} and \mathbf{b} in equation 2.5, and minimize the error of predictions, we first need a cost function similar as the one for linear regression that measures the error between the predicted values and the training data. For regression problems, we use MSE as the cost function for neural networks, which is the same cost function we used in linear regression. For classification problems, cross-entropy is the cost function that is widely used. The algorithm that is widely used for training neural networks is called backpropagation training algorithm [34]. Backpropagation algorithm used two steps and gradient descent repeatedly to minimize cost function's value [30]. In the first step, the algorithm computes the prediction and measures the prediction error by feeding the input features forwardly from

the input layer to the output layer, which is called the forward pass. In the second step, the algorithm goes in reverse from output error to the input layer to compute the gradients of cost function corresponding to every connection weight, which is called the backward pass. Finally, the gradients computed will be used in the gradient descent, which was mentioned in section 2.6.1, to change weights of neural networks to reduce cost function's value.

Neural networks are non-parametric machine learning models that are powerful to learn highly nonlinear relationships in high-dimensional data [12, 11], which is suitable to model complex relationships lying in transportation datasets. Because of their advantages and ability to make accurate predictions, neural networks are widely used in scientific and industrial applications, e.g., computer vision, natural language processing, and transportation applications such as traffic forecasting.

Chapter 3

Related Work

This chapter introduces related studies in data-driven traffic flow estimation using mobile data and the works in traffic data imputation.

Previous studies in data-driven traffic flow estimation using mobile data mainly focused on extracting the relationships between traffic flow and other traffic variables lying in stationary historical data using statistical or machine learning models. After the relation model is trained/calibrated, streaming mobile data is used as input to estimate the traffic flow.

Blandin et al. [7] and Bulteau et al. [8] used linear regression to fit FD-like relations between traffic flow and speed/speed variance in uncongested states. Wilby et al. [35] also proposed a method that utilized linear regression to model the relations between flow and traffic variables collected from extended floating car data for different traffic regimes, e.g., free-flow and congested traffic. However, the approaches proposed by these works require either manually identification or computationally complex algorithms to determine the segmentation thresholds between different traffic conditions/regimes, which are not scalable traffic estimation solutions. The linear models are also not suitable for multivariate modelling, which incorporates multiple dependent variables for estimation and should benefit from the increasing data sources emerging from the Internet of Things. Anuar et al. [5] used multiple FD functions from traffic flow theory to fit the flow-speed relationships in a stationary dataset. The authors then derived the traffic flow from mobile data speed and compared the estimation accuracy corresponding to each fitted model. The model proposed by this work is more restrictive to the functional forms that were chosen by authors for fitting the flow-speed relationship than other data-driven approaches. TSE approaches mentioned above used stationary relationships between two traffic variables

for estimation, which cannot capture the temporal or spatial dependency of dynamic relationships mentioned in section 2.5 .

Some studies tried to model the dynamic relationships between traffic variables when developing their estimation models. Neumann et al. [6] proposed a stochastic approach to model the dynamic flow-speed relationship by using Bayesian networks and used the models to estimate the traffic flow from mobile data, speed, in a wide area. The approach considered the temporal dependencies and transitions between traffic states when extracting the relationship from the historical dataset. Antoniou et al. [27] proposed a non-parametric ML-based approach that incorporated multiple traffic variables for estimating speed. Although this approach was not developed for estimating flow but for estimating speed from density and flow, it could also be used for flow estimation from traffic variables collected from mobile sensors. The proposed estimation approach used a combination of several ML methods, including k-means clustering, locally weighted regression, and **K-Nearest-Neighbor (KNN)** classification. It also can capture the dynamic relationship between traffic variables and the change in traffic conditions. The study is also one of few studies, to the best of author's knowledge, that used multiple traffic data as dependent variables, i.e., input features, for estimating the traffic state. However, the ML methods used in this work are not suitable for modelling datasets with high dimension, i.e., the number of feature variables, and large size, i.e., the number of instances in the dataset. For example, k-means clustering and KNN classification both suffering from the "Curse of Dimensionality", which means they do not perform well in high-dimensional data. k-nearest-neighbor also needs long computational time to classify an instance when the size of the training dataset is large because the computational complexity of KNN is proportional to the number of instances in the dataset. Besides, some model-driven TSE approaches were developed to capture the time-varying traffic conditions by updating the model parameters dynamically, i.e., on-line calibration [26, 36].

Compared with previous works of data-driven TSE using mobile data, the approach proposed in this work is highly automated and simple to implement, with no need for human intervention in model building. The proposed neural network model captures traffic flow relationships' temporal and spatial dependency to make more accurate flow estimations. Besides, thanks to the neural network's ability to capture complex relationships between data variables in a high dimensional dataset, the proposed approach is flexible to incorporate various available information, e.g., travel time, as input features in addition to the single traffic state variable for estimation.

On the other hand, previous works in imputation, a type of TSE for imputing missing traffic data in datasets, also deserve mention because our approach could also estimate the missing data of flow on road segments where fixed sensors are installed but suffer from temporary malfunctions. The imputation methods could be classified into three categories: the prediction, interpolation, and statistical method [4, 37].

Prediction methods apply the approaches for traffic forecasting in imputation. They view the missing data as a traffic state to be predicted in the future using the previous data points in the same time series. They usually learn or calibrate the temporal relationship between a data and its previous data, i.e., data in several previous timestamps, in a time series from the historical datasets. Some popular time-series approaches used in prediction methods are **Autoregressive Integrated Moving Average (ARIMA)** and ANN [4].

Interpolation methods use the same sensor's historical data or neighboring data points to replace the missing/corrupted value. There are two types of interpolation methods widely used for imputation: the temporal-neighboring method and the pattern-similar method. The temporal-neighboring methods use the average value of historical data in the same time period from neighboring days collected from the same sensor to impute missing data [38]. The method is based on the assumption that traffic flow patterns on roads are regular and rarely change from the previous day. The temporal-neighboring method is strict in data usage because it only uses historical data in the same time period from the neighboring days for imputation, which is therefore known as the history model. It could quickly fail when the pattern of traffic flow changes between days, e.g., the difference between weekdays and non-weekdays. On the other hand, the pattern-similar methods impute the missing data using historical data from the same sensor but from the days with similar data patterns when the data is missing. A classic technique used in pattern-similar methods is **KNN** [39]. It is more flexible than the temporal-neighboring method because data is not confined to the neighboring days but from a broader range of historical data having similar patterns.

Statistical methods usually first develop a probability distribution model, then train the model parameters and impute the missing data at the same time using historical data [37]. A classic statistical method is Markov Chain Monte Carlo imputation method [40].

Recently, deep learning methods are widely used for traffic imputation and have achieved better imputation performance than traditional methods [4, 37]. The fundamental idea of deep learning-based methods is to use neural networks to capture the temporal and spatial information from a large-

scale dataset containing neighboring data in time and space. Duan et al. proposed a deep learning model called denoising stacked autoencoders for traffic flow imputation [4]. The model captures the pattern features and correlations from a high-dimensional dataset containing flow data collected from various detectors and different weekdays during a whole year. Zhuang et al. adopted the image inpainting approach widely used in computer vision for traffic data imputation [37]. The method first transforms the raw volume data collected from nearby detectors into two-dimensional temporal-spatial images. It then trains a **Convolution Neural Network (CNN)** based encoder-decoder to impute the images with missing parts via learning the high-level features in the temporal-spatial images. Both deep learning methods showed better imputation performance than classic methods such as the history model, **ARIMA**, and state-of-the-art statistical model [4, 37].

When compared with the imputation works, our approach could be regarded as a flow data imputation approach using alternative data sources. The method we use is slightly similar to the history model. However, instead of using average values from historical data to impute the missing data, we use average "traffic flow relationships" in the same period from the historical data and the real-time mobile data as input to infer the missing data. Moreover, the approach solves the history model's bad performance problem on non-weekdays by incorporating the temporal factor denoting different weekdays to capture different traffic flow patterns between weekdays and non-weekdays. To the best of the author's knowledge, very few imputation works use alternative data sources to impute the missing or corrupted flow data. One benefit that our approach brings is that the imputation performance would be less affected by the missing ratio than many imputation methods [37]. It is because our approach does not rely on the missing data point's neighboring data for imputation.

Chapter 4

Datasets and Methodology

This chapter provides an overview of the datasets and the methods used in the thesis project. We first describe the two traffic datasets on which the project is built. The remaining sections then present the processes and techniques we adopted during the project's implementation, including data preparation, model structures and training, and evaluation metrics.

4.1 Datasets

Traffic data provided by two sensor platforms are used to train and test the estimation models in the thesis, i.e., the INRIX and the Motorway Control System (MCS). INRIX datasets belong to the mobile data, while MCS datasets are a kind of stationary data introduced in section 2.2. The data are collected from two consecutive road segments on the four-lane E4 highway, southbound, in Stockholm from 2018-10-01 to 2018-10-31. Figure 4.1 shows the locations of INRIX road segments and MCS sensors on the map. Table 4.1 lists the IDs for INRIX road segments and MCS sensors in the datasets. We use "south" to denote segment 1071883675 and sensor 1159 and use "north" to denote segment 225285973 and sensor 1162 in the thesis.

Road Segment	INRIX ID	MCS ID
South	1071883675	1159
North	225285973	1162

Table 4.1 – INRIX ID and MCS ID for corresponding road segments.

The first three weeks of data, i.e., 1st to 21st October, are used as training

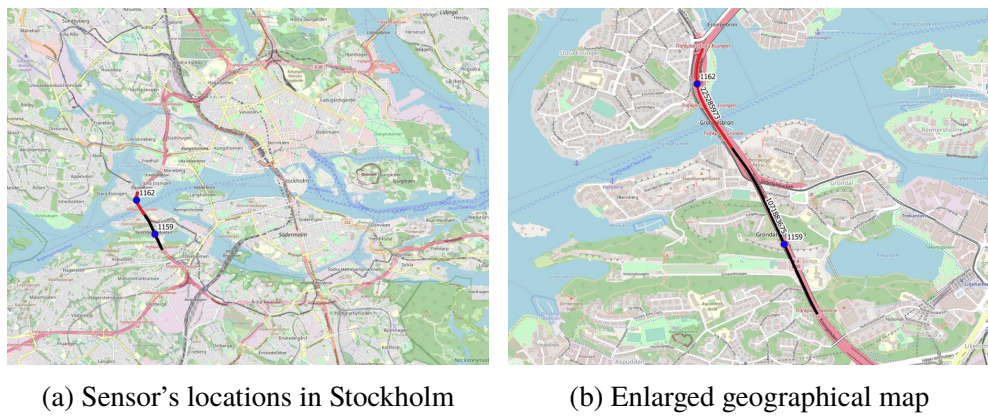


Figure 4.1 – Locations of INRIX segments and MCS sensors in Stockholm.

datasets for building/training each estimation model, and the following one week of data, i.e., 22nd to 29th October, from both road segments are used as test datasets for evaluating the application of the models. Both platforms provide aggregated traffic measurements, timestamps, and other traffic-related information at a frequency of once every minute, and both data are delivered in **Comma-Separated Value (CSV)** format. Detailed information about two data sources and the traffic information they provide is presented in the following sections.

4.1.1 INRIX

INRIX combines data from many sources to provide traffic information. A major part of the data comes from a crowdsourced model where INRIX continuously collects speed and location from probe vehicles, combines the data into an updated view of the current traffic situation on the road, and sends it back to the vehicles. In a press release in May 2010¹, INRIX said they had a network of two million GPS-enabled vehicles: “*Providing a foundation of continuous real-time speed and location reports to INRIX every minute for an average of 7 hours per day, per vehicle, commercial fleets – such as taxi cabs, service delivery vans and long haul trucks – represent the majority of INRIX’s network. INRIX intelligently combines these reports with data from consumer vehicles and GPS-enabled smartphones to deliver a service that updates traffic information to drivers every minute, ensuring they have the most accurate view of traffic conditions wherever they go.*”

¹ "INRIX's Crowd-Sourced Traffic Network Surpasses 2 Million Vehicles", INRIX press release, May 5, 2010. <<https://inrix.com/press-releases/2650/>>, viewed 5 June 2020.

Table 4.2 shows the schema and an example of data from the INRIX dataset. Data fields in bold in table 4.2 are the variables of interest in the project.

Field	Description	Example
Segment ID	An identifier for defining a unique road segment.	1071883675
Timestamp	The timestamp of the measurement in UTC.	2018-10-01 00:00:12
Segment Type	Type of road segment: XD Segment (XDS) or TMC segment.	XDS
Speed	Average speed of vehicles on the segment calculated from the most current time slice, in km/h.	93
Average Speed	The historical average speed on the segment for the given day and time (km/h).	68
Reference Speed	An expected free-flow speed on the segment, determined from the INRIX traffic archive (km/h).	68
Travel Time	The time required to travel across the segment in minutes.	0.738
Score	A measure of confidence in a given reported speed with three possible values: 10/20/30 [18]. Samples with confidence score larger than 10 are based on real-time data, otherwise are based on historical data.	30
Cvalue	The second measure of confidence ranges from 0 to 100, which only applies when the confidence score is 30 [18].	49
Speed-bucket	Level of congestion according to the range of speed.	3

Table 4.2 – The schema and example of the INRIX dataset

To be noticed that the speed reported by INRIX every minute is space-mean speed calculated from the most current time slice [17]. In the thesis project, speed and/or travel time are used as main input features for estimation models. In contrast, timestamp and segment ID are used for preparing

temporal and spatial factors in the feature vector for capturing time and space dependency of the traffic relationship.

4.1.2 Motorway Control System (MCS)

The traffic flow in Stockholm is monitored with the [Motorway Control System \(MCS\)](#) by the Swedish transport administration (Trafikverket). Many stationary MCS-portals have been installed on the gantries on the E4 highway and other roads in Stockholm's road network. The MCS-portals are equipped with radar sensors, which monitor the traffic flow and speed in each lane of the road every minute. The data provides the regional traffic control center with information about the current traffic flow and speeds. The data is also input to a control system that sets variable speed limit signs.

Field	Description	Example
Fk_id	Reference ID identifying the location of sensor on the road.	1159
Timestamp	The timestamp of the measurement.	2018-10-01 00:01:00
Speed	Average speed of vehicles passing the sensors in the past minute, in km/h.	93.816
Flow	Flow rate in veh/h, calculated from the number of vehicles passing the sensors in the past minute.	160
Used Lane	The lanes contribute to the measurements in the past minutes. NULL indicates there are no vehicles on the lane.	1,1,1,NULL

Table 4.3 – The schema and example of the MCS dataset

The distance between the locations of two MCS sensors in this work is 1 km. The MCS measurements are aggregated over a minute while reported by the system. MCS measurements are fixed-point measurements and hence provide time-mean speed as reported speed after aggregation. On the other hand, the probe measurements such as INRIX calculate the space-mean speed over a road segment as vehicles' reported average speed [17]. Different measurement techniques also lead to bias and delay in INRIX data compared to stationary sensor speed [17, 18]. To be noticed that the MCS datasets used

in this project have been further aggregated over raw sensor data from all lanes on E4 to obtain average flow and speed on the road.

The schema of the MCS datasets and an example from the south segment are shown in table 4.3. Data fields in bold are the variables selected and used in the project. The traffic flow in MCS datasets is used as labels for training and testing the project’s estimation models. On the other hand, we use MCS speed data as a benchmarked speed for mitigating the latency exhibited by the INRIX data during the data preparation.

4.2 Data Preparation

Various data exploration and preparation techniques are adopted to prepare the datasets, including feature vectors and labels, to train and test the estimation models. Techniques such as plotting and statistical measures, e.g., correlation coefficient, are used in the explorative analysis to get insights into the datasets and evaluate the effect of data preparation on the variables. Regarding data preparation, the following techniques of feature engineering for machine learning are adopted for preparing the datasets:

- **Filtering:** The INRIX datasets contain data points with a low confidence score (10), which always report the same speed value equals the historical reference speed, and thus cannot reflect the real-time traffic condition on the road segment. We filter out these data points in INRIX datasets to ensure the traffic variable values represent the traffic condition at the moment of measuring.
- **Smoothing:** The measurements of traffic variables, i.e., flow, speed, are noisy in INRIX and MCS datasets. We need to remove noise and expose the variable values that signify the real trends to increase the models’ estimation accuracy. Moving average with a window width of 30 time-steps is adopted for smoothing the speed, flow, and travel time.
- **Shifting:** A 6-minute latency of speed is observed in INRIX datasets compared with the MCS speed. This lag-time is within the latency range, from 6 to 8 min, reported by various studies [18]. We eliminate the latency by shifting the INRIX time-series by 360 s to ensure the measurements from both types of datasets reflect the same traffic condition in the same timestamp. Besides, INRIX and MCS’s timestamps were registered in different time-zones, requiring time-series shifting to match the timestamps from two platforms beforehand.

	Timestamp, Segment ID	2018-10-03 20:21:00, 1071883675
One-hot Encoding	hour feature [00, 01, ..., 23]	[0, 1, 0, 0, 0, 0]
	day feature [weekday, weekend]	[1, 0]
	location feature [south, north]	[1, 0]

Table 4.4 – Example of one-hot encoding features for temporal and spatial factors.

- One-hot Encoding: One-hot encoding [30] is adopted to convert INRIX's timestamps and segment IDs into time-related features and space-related with a numerical form for ANN models. We prepare two time-related features and one space-related feature to help estimation model extracting time and space-dependent traffic relationships:

hour feature: the hour "part" in the timestamp is converted into a 24-bit one-hot code, which represents the hour of observation in a day.

day feature: the "day" part in the timestamp is converted into a 2-bit one-hot code, representing the day of observation in a week, i.e., on weekdays or weekends.

location feature: the "segment ID" is converted into a 2-bit one-hot code, representing the location of the observation on the E4, i.e., on the south or north segment.

Table 4.4 shows an example of one-hot encoding time and space features for an INRIX data point measured at 20:00 Wednesday on the south segment, together with its original timestamp and segment ID.

- Feature Scaling: A machine learning model's input attributes need to be on the same scale for the machine learning algorithm to perform well. Two methods are commonly used to scale the input attributes, i.e., normalization and standardization. We adopt standardization to scale the numerical attributes for neural networks, i.e., speed and travel time, because it is less affected by the outliers in datasets than the normalization. Standardization first subtracts the mean value of the dataset from the feature values, then divides them by the standard deviation, as shown in equation 4.1. The standardized input attribute

has a zero mean and a unit deviation in its distribution.

$$x' = \frac{x - \bar{x}}{\sigma} \quad (4.1)$$

x' = the standardized input feature x = the original feature

\bar{x} = the mean of the feature values

σ = the standard deviation of the feature values

4.3 Models

Our goal is to develop an approach that automatically finds relationships between observed variables in INRIX data and the flow in MCS data, which can later be used for estimating un-observed flow from the INRIX data collected in the future and the neighboring area. These relationships are the flow estimation models which we are going to train and test using prepared datasets. Two types of models are trained in this work: a multi-regime baseline model and ANN models. The multi-regime baseline model acts as a benchmark for comparison with the ANN models proposed, while ANN models are built for the purposes listed in section 1.3.

4.3.1 Baseline Model

Multi-regime models are widely used for modeling the relationships of traffic variables [3, 7, 27, 41], which use different functional forms for modeling the relationships in different traffic conditions in FDs. Many studies used linear regression to describe the linear relationship between flow and speed in the free-flow condition [7, 41]. When the speed becomes slower and the traffic condition becomes dense or even congested, curved relationships between flow and speed are often observed in the samples. Some studies adopted the functional form derived from the linear flow-density relationship based on equation 2.1 to describe the dependency between flow and speed under this condition [7, 41].

In this work, we build a multi-regime model as the baseline model to capture the classic static flow-speed relationship using data in the south segment's training dataset. This baseline model will be used to compare the proposed ANN models, which incorporate various additional factors such as temporal and spatial dependencies into the estimation. The mathematical

expression for the baseline model is shown in equation 4.2. As shown in equation 4.2, we set a threshold speed of 70 km/h to separate the samples into free-flow and non-free-flow conditions. We use linear regression to capture the relationship between traffic flow and speed for the samples with speed higher than the threshold speed. When the sample's speed is lower than the threshold speed, we assume that the traffic condition on the road is not in the free flow anymore, and the flow-speed relationship is modeled using a second-degree polynomial regression determined by the hyperparameter tuning.

$$\hat{q} = \begin{cases} av + b & \text{if } v > v_t \\ cv^2 + dv + e & \text{otherwise} \end{cases} \quad (4.2)$$

$$\begin{aligned} \hat{q} &= \text{estimated flow} & v &= \text{speed} & v_t &= \text{threshold speed} \\ a, b, c, d, e &= \text{model parameters} \end{aligned}$$

We determined the threshold speed of the free-flow condition based on two reasons. The first reason is, the speed limit on the road segment where our data collected is 70 km/h. Thus, if the vehicle's speed is slower than the speed limit, we assume that the drivers cannot drive freely due to increased vehicle density and influences from other vehicles. The second reason is that we observed a clearer transition point around 70 km/h between the two traffic conditions with different flow-density relations in the flow-density curve when we plotted the flow-density FD based on the relation in equation 2.1 [7, 41].

4.3.2 Neural Network Models

The project aims to develop model structures that produce accurate flow estimation results from INRIX data by utilizing the neural network's ability to learn and model high-dimensional and non-linear relationships. We construct five neural network models to evaluate the neural network's performance in modeling classic flow-speed relationship, the relationship between traffic flow and multiple input features, and time-space-dependent relationships using prepared datasets.

All proposed neural networks are based on an architecture called "Wide & Deep Learning," introduced in a 2016 paper [42]. The architecture enables ANN to learn both deep patterns through deep neural network layers and simple patterns in data by connecting the inputs directly to the output layer [30, 42]. Each neural network consists of six layers: one input layer, three hidden layers, one concatenate layer and one output layer. The first layer is

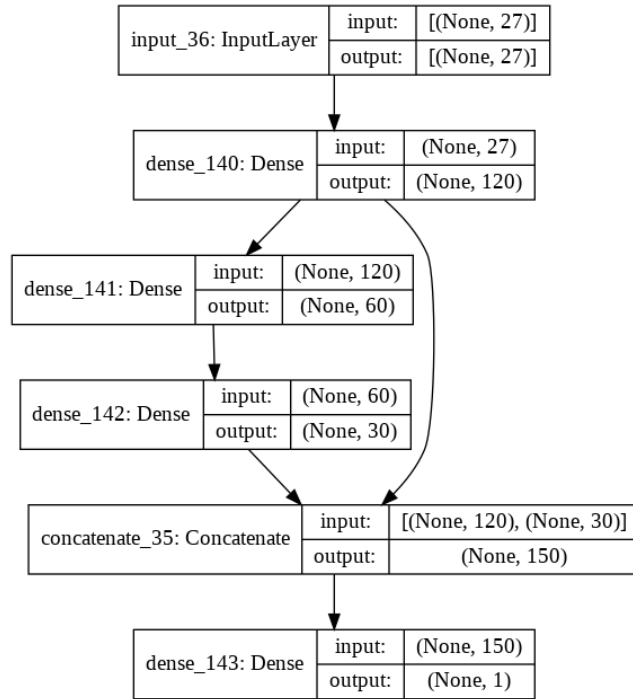


Figure 4.2 – Structure of the neural network considering temporal dependencies.

an input layer with dimension n equals to the number of input features. For example, if the model's independent variables are speed and travel time, n equals two. The input layer is followed by three densely connected hidden layers containing 120, 60, and 30 neuron nodes, respectively. The number of neuron units in each hidden layer is determined by hyperparameter tuning. The first and third dense hidden layer outputs are fed into a concatenate layer, which merges the outputs of two layers and feeds the concatenation to the output layer. The purpose of the concatenate layer is to provide a short path to the model, through which it can learn simple and undistorted patterns from the layer closer to the input features. The last layer of the model is an output layer, which densely connects its inputs and produces a predicted value of traffic flow on the road segment as the entire estimator's output. The dimension of the output layer is one for all neural network models. Figure 4.2 shows the structure of one of the proposed ANN models with 27 input features, including speed, hour, and day features, which are listed in table 4.4.

"None" in input and output shapes in figure 4.2 means the number of samples in the data batch is not fixed but flexible for different datasets. We use MSE as the cost function and Adam algorithm, an extension of gradient

descent algorithm, as our optimization algorithm for training the neural networks. More details about each neural network and its corresponding purpose are presented as follows.

Univariate Neural Network

The ANN model characterizes the simple flow-speed relation with a single independent variable, speed. The mathematical representation of the estimation model is shown as equation 4.3.

The purpose of this univariate neural network is to evaluate ANN's ability to learn and model the stationary flow-speed relationship from the data compared with the traditional baseline model. The model is trained on the INRIX speed and MCS flow in training datasets collected from the south road segment from 1st to 21st October. In order to evaluate the model's estimation accuracy and its generality for the adjacent road segment, we test the model on the test datasets, as mentioned in section 4.1, collected from both the south and north segments in the following week.

$$\hat{q} = E(v) \quad (4.3)$$

$$\hat{q} = \text{estimated flow} \quad v = \text{speed}$$

Multivariate Neural Network

We incorporate travel time, another real-time information of road traffic provided by INRIX, as an additional feature for flow estimation. The multivariate neural network with two input features, speed and travel time, is constructed to evaluate ANN's ability to capture non-linear relationships between multiple traffic variables, which is a more complicated task when only using linear regression. Moreover, the model is used to evaluate whether the travel time is a useful feature that can provide additional information than speed to improve the estimation accuracy.

$$\hat{q} = E(v, tt) \quad (4.4)$$

$$\hat{q} = \text{estimated flow} \quad v = \text{speed} \quad tt = \text{travel time}$$

Neural Network with Temporal Dependency

A neural network that considers the temporal dependency of the flow-speed relationship is constructed. The neural network incorporates time-related features, i.e., hour and day features introduced in section 4.2, as its inputs to capture the dynamic flow-speed relationship, which changes with different hours in a day and different days in a week. The structure of this neural network was already shown in figure 4.2, and the mathematical representation of the model is shown as equation 4.5. To be noticed that the hour feature is a 24-bit one-hot encoding representing each hour in a day, and the day feature is a 2-bit one-hot encoding representing weekday or weekend. Therefore, the model has an input vector with a dimension of 27. The model is also trained on south segment data and tested on data from both road segments in the following week.

$$\hat{q} = E(v, h, d) \quad (4.5)$$

$$\begin{aligned}\hat{q} &= \text{estimated flow} & v &= \text{speed} & h &= \text{hour in a day} \\ d &= \text{day in a week (weekday or weekend)}\end{aligned}$$

Multivariate Neural Network with Temporal Dependency

Like the multivariate ANN, this neural network incorporates travel time in addition to the speed as the second input feature. The difference is that this ANN also considers the temporal dependency of traffic conditions by incorporating the time features, i.e., hour and day.

The purpose of this model is to examine whether the travel time as an additional independent variable can improve the estimation accuracy when the model also captures the transitions of the traffic conditions over time.

$$\hat{q} = E(v, tt, h, d) \quad (4.6)$$

$$\begin{aligned}\hat{q} &= \text{estimated flow} & v &= \text{speed} & tt &= \text{traveltime} \\ h &= \text{hour in a day} & d &= \text{day in a week (weekday or weekend)}\end{aligned}$$

Neural Network with Spatiotemporal Dependency

Finally, we construct a neural network considering both temporal and spatial dependencies when modeling the flow-speed relationship. The model is trained on data from both road segments, i.e., south and north, with time-

related input features, i.e., hour and day, and a 2-bit location feature that identifies the road segments. Same as other models, the model is tested on the data collected from both road segments in the following week. In general, the flow-speed relationship varies with time and locations in a road network [7]. The purpose of this neural network is to evaluate ANN's ability to learn complex spatial and temporal dependencies of relationships between traffic variables for multiple road segments. The model shows the possibility of building a central estimation model that can learn the spatiotemporal dependencies in the entire road network and estimate the traffic flow for road segments between fixed sensors using ANN, reducing the number of models needed.

$$\hat{q} = E(v, h, d, l) \quad (4.7)$$

\hat{q} = estimated flow v = speed

h = hour in a day d = day in a week (weekday or weekend)

l = location (south or north)

4.4 Performance Evaluation

In this work, the Root Mean Square Error (RMSE) and the Mean Absolute Percentage Error (MAPE) are used to evaluate the trained estimation models' accuracy when applied to the test datasets. Both RMSE and MAPE are popular evaluation metrics for traffic predictors and estimators [5, 8, 35].

$$RMSE = \sqrt{\frac{\sum_{i=1}^m (\hat{y}^i - y^i)^2}{m}} \quad (4.8)$$

$$MAPE = \frac{1}{m} \sum_{i=1}^m \left| \frac{y^i - \hat{y}^i}{y^i} \right| \quad (4.9)$$

In equation 4.8 and 4.9, y^i and \hat{y}^i is the observed value and estimated value of the i^{th} sample, respectively, and m is the number of the samples. RMSE measures the differences between values predicted by an estimator and the actual value, i.e., the prediction errors, and computes the square root of the average of squared errors. RMSE is also a straightforward measure that has the same unit as the predicted variable, i.e., veh/h in this thesis. On the other hand, MAPE expresses the accuracy as a “percentage error” by computing the

average of absolute ratios of prediction error to the actual value. The MAPE in the project is presented in percentage after multiplying by 100%.

Chapter 5

Results

This chapter presents the results of implementation and the validation of flow estimation models introduced in chapter 4. Three sections of this chapter describe data preparation results, model training results, and traffic flow estimation results using proposed models.

5.1 Data Preparation Results

Figure 5.1 shows the time-series INRIX speed and MCS flow in 1st October, from the south segment, before and after the moving average smoothing with a window width of 30 minutes. Smoothing removes noises in the data and exposes the underlying trends of the traffic state variables over time. Smoothing also makes it easier for the estimation model to capture the relationships between flow and speed from the noisy INRIX and MCS data.

Figure 5.2a presents the INRIX speed and MCS speed versus epoch, i.e., cumulative time, based on their original timestamps. We can observe an approximate 6-minute latency of INRIX speed compared with the MCS speed from the figure, which is a common phenomenon reported by various studies related to the INRIX data [18, 17]. Since we aim to develop the relationship models that mapping the INRIX variables to the MCS flow and then use the models to estimate the traffic flow, we do not want any time difference between INRIX and MCS's observations. Therefore we shift the INRIX timestamps by 360 s to remove the time-lag between two measurements. Figure 5.2b presents the time-series INRIX and MCS speed after the timestamp shifting. We can see that the time-lag is disappeared, and the two curves overlap better after the shifting. By removing the latency, we ensure that both sensor platforms' measurements with the same timestamp reflect the same traffic condition at

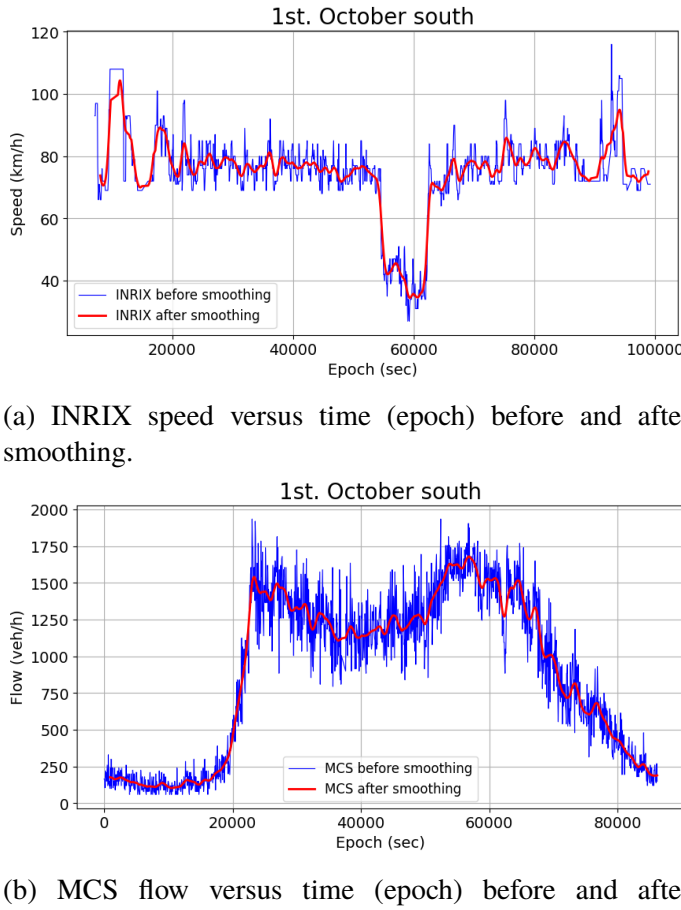


Figure 5.1 – Time-series INRIX speed and MCS flow before and after smoothing on 1st October.

that moment.

Figure 5.3 presents box-plots showing the distributions of speed in the training and test datasets collected on both road segments before and after feature scaling, i.e., standardization. From figure 5.3, we can see that the north segment's median speeds before the standardization are approximately 3 km slower than median speeds on the south segment, whether in the training sets or test sets. One reason for the lower median speed on the north road segment is that the north segment, compared with the south segment, is closer to Stockholm's city center, which generally has lower speed limits and more traffic than the city's outer parts. The interquartile ranges of the speed values are similar on both road segments. Figure 5.3 also shows the distributions of standardized speeds in each dataset. We can see that the median values and

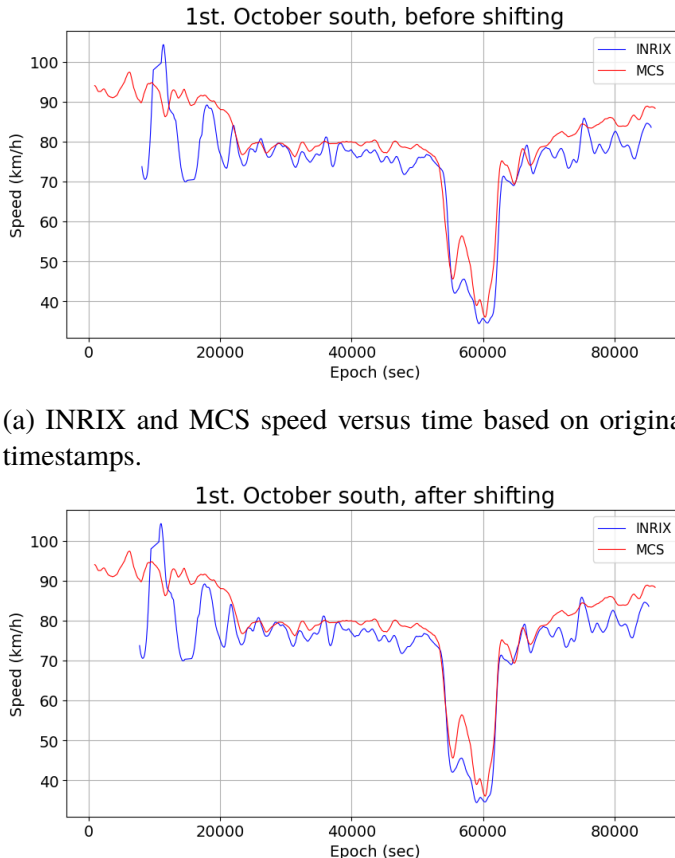


Figure 5.2 – INRIX and MCS speed versus time (epoch) before and after shifting INRIX timestamps on 1st October.

the interquartile ranges on both road segments are similar. As standardization subtracts the historical mean speed value from the original speed value, the standardized speeds have a mean value close to zero. Thus the difference of median speed between the north and south segments is reduced.

On the other hand, the distribution of speed in the test set is similar to the distribution in training set on the same segment, which means that the speed behavior did not change much in the short term future of one week.

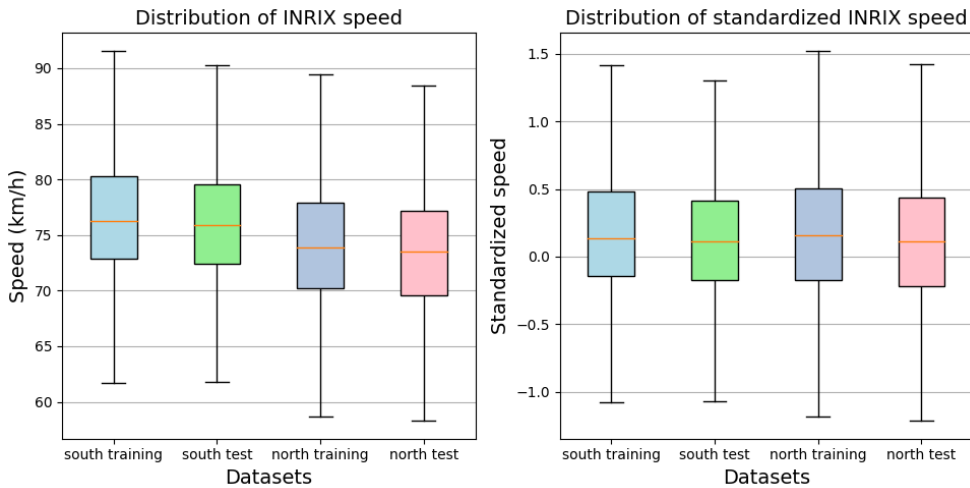


Figure 5.3 – Distributions of INRIX speed in training and test datasets before and after the standardization.

5.2 Model Training Results

Figure 5.4 shows the baseline and the ANN flow-speed relationship trained on the samples from the south segment's training set. The samples used for training are also presented in the figure for comparison with the relationships. To be noticed that the threshold speed separating the free-flow from the saturated regime for the baseline relationship in figure 5.4 is 70 km/h. The threshold speed was determined from the flow-density diagram using a regime identification method from [41]. The density values were inferred from the flow and speed values using the equation 2.1. Training errors for both models are shown in the table 5.1.

Training Error	Baseline Model	ANN Model
MAPE	96.49%	87.61%
RMSE	385.23	372.61

Table 5.1 – Training errors for baseline and univariate ANN flow-speed relationship model.

Generally speaking, the ANN flow-speed relationship fits the training samples better than the baseline model, especially in the free-flow regime. From figure 5.4, we can see that the baseline model uses linear regression to fit the samples in the free-flow regime, which is a common method for fitting

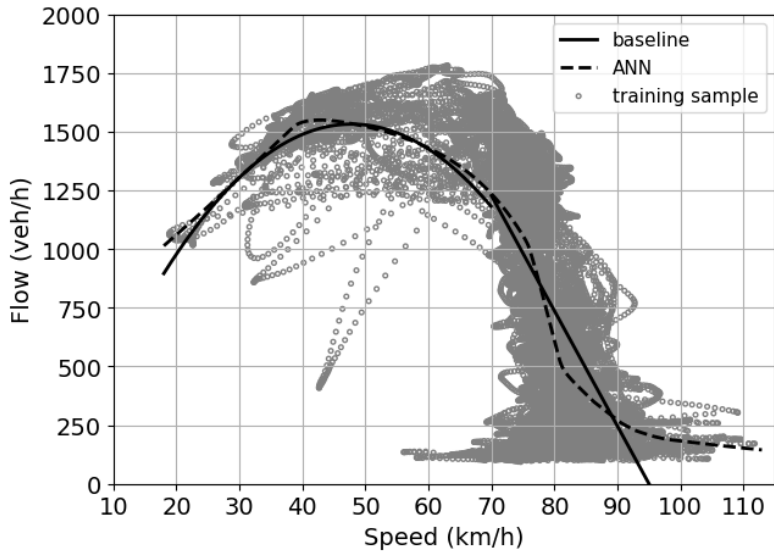


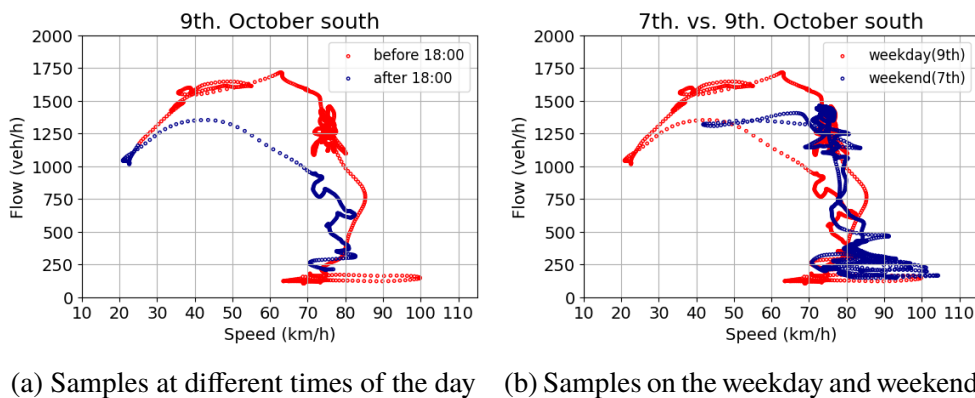
Figure 5.4 – Baseline versus univariate ANN flow-speed relationship.

the flow-speed relationship in free-flow regime [7, 41]. However, the flow-speed relationship in the free-flow regime is more S-shaped than linear in our dataset. ANN as a non-parametric model without fixed functional forms can adapt itself to the data and better fit the S-shaped flow-speed relationship in the free-flow regime. The ANN also has an advantage in the high-speed region, i.e., speed is larger than 90 km/h, where the traffic flow is low and barely changes with the speed.

Although the ANN can model the flow-speed relationship better than the baseline model, it does not mean that there is no space to improve our estimation model. In figure 5.4, we can see that relationship between flow and speed is not deterministic; each speed value usually corresponds to a wide range of flow values in the samples. For example, when the speed is 80 km/h in the free-flow regime, the flow ranges from about 100 veh/h to 1500 veh/h, near eighty percent of the entire flow range! As we mentioned in the previous section, the flow-speed relationship varies over time rather than stationary. Thus, a deterministic curve could not capture the traffic flow variation given the same speed under different traffic conditions over time. One way to tackle this problem is to model the dynamic relationship using stochastic statistical models, e.g., Bayesian networks, which consider the transition between traffic conditions over time [6].

Another method to capture the dynamic flow-speed relationship on a road segment is to represent the flow-speed relationship as a time-varying function

that considers temporal factors, e.g., time of a day, as features that affect the relationship curves. Figure 5.5 shows flow-speed behaviors of training samples in different time segments. In figure 5.5a, samples' distributions are different during different time segments of a day. For example, the traffic flow drops after 18:00 as compared with the earlier traffic states during the rush hours given the same speed. Weekdays and weekends also exhibit different behavior of flow-speed relationship. Figure 5.5b shows the training samples collected on Sunday (7th) and Tuesday (9th) on the same road segment. In figure 5.5b, we can see that the shape of relationship curves is different on the weekend from a weekday. The traffic flow on weekdays and weekends could significantly differ given the same speed in some time segments, e.g., morning.



(a) Samples at different times of the day (b) Samples on the weekday and weekend.

Figure 5.5 – Training samples' different flow-speed behaviors in different time segments.

By incorporating temporal factors as input features, we could train our ANN model to learn the dynamic flow-speed relationship over time. Figure 5.6 presents the trained ANN model considering temporal dependency, whose input features include speed and two time-related features, i.e., a 24-bit hour feature and a 2-bit day feature, as shown in equation 4.5. Instead of learning one static flow-speed relationship for the entire time, the temporal ANN learns many micro-relationships during training; each corresponds to a different time segment, i.e., a different hour of a day and a different day of a week. By incorporating additional time-related features, our ANN estimation model can capture traffic flow variation given the same speed to a certain degree. For example, the model will not provide only one estimated flow value when the speeds equal 80 km/h, but estimate the traffic flows according to which hour of a day and which day of a week sample's speeds are measured. Temporal ANN fits the training samples much better than the baseline and univariate

ANN models, which are static flow-speed relationships. The temporal ANN's training MAPE is 11.54%, and RMSE is 92.41. Most importantly, ANN learns and captures all micro-relationships for different time-segments automatically and efficiently without the need for human intervention or tedious codes for automation.

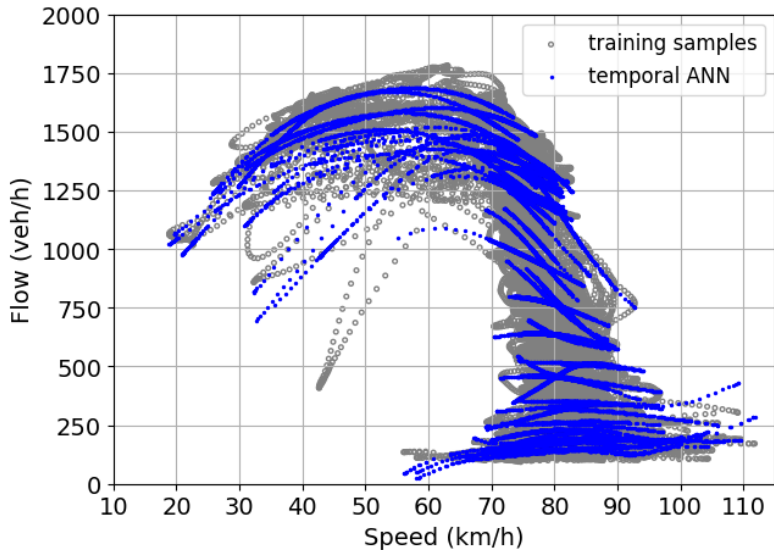


Figure 5.6 – Temporal ANN model considering flow-speed relationship's dependencies to the hour of a day and the day of a week.

As mentioned in the previous section, the traffic condition depends on many factors, e.g., weather and lighting conditions, vehicle composition, road surface, and driver characteristics [2, 36], all of which may affect the flow-speed relationship. Using temporal segmentation could not accurately capture the dynamic transitions between traffic conditions because they do not always occur during the changing of hours. Representing the traffic relationship as a time-varying function can also not reflect some causes leading to the changes of traffic conditions over time, e.g., percentage of the trucks. However, Incorporating the temporal dependency into the estimation model is a practical method to capture the dynamics of flow-speed relationships because it is difficult to explicitly monitor every factor on the road that affects the traffic conditions. We can see that this method effectively improves the model's training accuracy to a satisfactory level on a road segment whose traffic conditions are relatively ordinary and recurrent. In addition to the above models, we trained the other three ANN models mentioned in the section models using the training datasets. Each of the models incorporates additional

features, i.e., travel time and location, for modeling the time-space-varying relationships between traffic state variables. In the next section, all estimation models are applied for estimating the traffic flows in unobserved time-space regions using the test datasets. Then we examine the overall performance obtained for each model.

5.3 Traffic Flow Estimations

Figure 5.7 represents the overview of the estimation performance in MAPE for all models when validated on the south and north test datasets collected in a week, i.e., 22nd to 29th, following the training dataset, i.e., 1st to 21st. However, before we start digging into each model's performance and comparing it with the baseline model, we observe a common phenomenon in the overall performance.

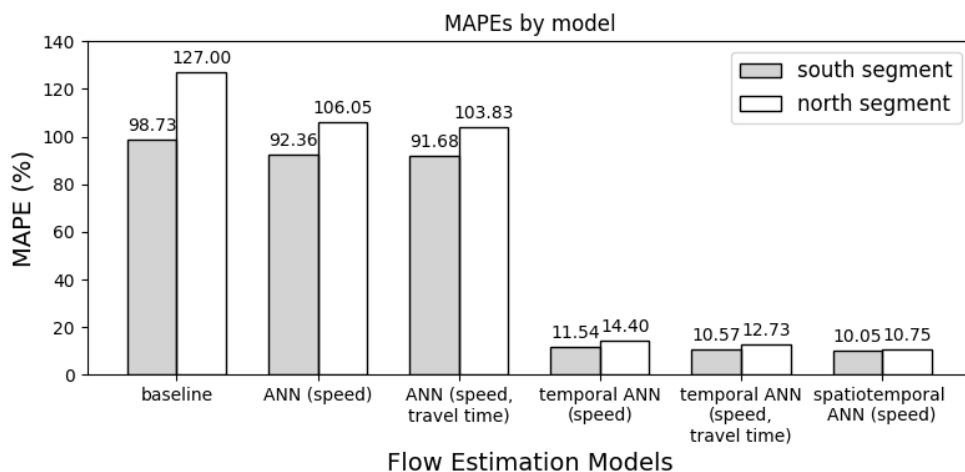


Figure 5.7 – Overview of the flow estimation performance on the two consecutive road segments.

Models generally perform better on the south segment, where the models were trained, than on its consecutive adjacent segment, i.e., the north segment, except the spatiotemporal ANN model on the rightmost. For example, the baseline model has a smaller MAPE of 98.73% on the south segment than the MAPE of 127.00% on the north segment. The reason for the phenomenon is quite straightforward. As traffic conditions depend on many space-related factors [2, 36], the traffic flow relationship on one segment may be slightly different from adjacent segments. Estimation models could perform well

on the segment where they were trained as long as the traffic condition does not change much in the short-term future, e.g., one week in our case. However, they may not perform well on the adjacent segments because the adjacent segments' traffic flow relationships could be slightly different from those learned by the models. Therefore, the models produce more accurate estimations on the south segment than on the north segment. However, as shown in figure 5.7, the degradation of estimation performance on the north segment could be mitigated using ANN as the estimation model, which will be discussed in detail later. On the other hand, the spatiotemporal ANN has similar MAPEs on both road segments because the model was trained on the samples from the both segments, which enable it to learn the unique traffic flow relationship for each segment.

The models in the figure 5.7 are presented from left to right with increasing complexity. The baseline model on the left is the simplest model with only one input feature, speed, and the spatiotemporal ANN on the rightmost is the most complex, having the most input features and model parameters. As shown in the figure, incorporating additional features and increasing the model complexity generally can improve the estimation performance on both segments. However, this trend is not always valid when evaluating the performance using RMSE, which we will see soon.

Tables 5.2 shows the improvements of ANN models as compared with the baseline model. We use the baseline model's MAPEs, i.e., 98.73% on the south and 127.00% on the north, as the reference performance to compare with the remaining ANN models. The ANN models can be categorized into three groups: The first group of ANNs considers only traffic variables, i.e., speed and travel time, as the independent variables without considering temporal or spatial dependency. The second group of ANNs considers temporal dependency in addition to the traffic variables, while the third group considers both the spatial and temporal dependency. The ANN using only speed as its independent variable has an improvement of 6.4% on the south segment and 16.5% on the north over the baseline model (south MAPE = 92.36%, north MAPE = 106.05%). Notice that ANN improves 10% more on the north segment over the baseline case than on the south segment, which means ANN can mitigate the notable performance difference between adjacent segments when using the baseline model for estimation. The reason for ANN's better generality on the adjacent road segments will be discussed in the following section. The ANN incorporates the travel time as an additional independent variable reaches an improvement of 7.1% on the south segment and 18.2% on the north, which slightly improves the previous univariate ANN on both road

MAPE(%)	Baseline		ANN		Temporal ANN		Spatiotemporal ANN	
	speed		speed		speed, travel time		speed	
	MAPE	improv	MAPE	improv	MAPE	improv	MAPE	improv
South	98.73	92.36	6.4%	91.68	7.1%	11.54	88.3%	10.57
North	127.00	106.05	16.5%	103.83	18.2%	14.40	88.7%	12.73
							90.0%	10.75
							91.5%	

RMSE(veh/h)	Baseline		ANN		Temporal ANN		Spatiotemporal ANN	
	speed		speed		speed, travel time		speed	
	RMSE	improv	RMSE	improv	RMSE	improv	RMSE	improv
South	380.98	373.56	1.9%	372.83	2.1%	96.81	74.6%	94.90
North	423.15	391.53	7.5%	397.97	6.0%	120.02	71.6%	104.36
							75.3%	87.71
							76.8%	79.3%

Table 5.2 – Improvements of flow estimation performance in MAPE achieved by ANN models over the baseline model.

Table 5.3 – Improvements of flow estimation performance in RMSE achieved by ANN models over the baseline model.

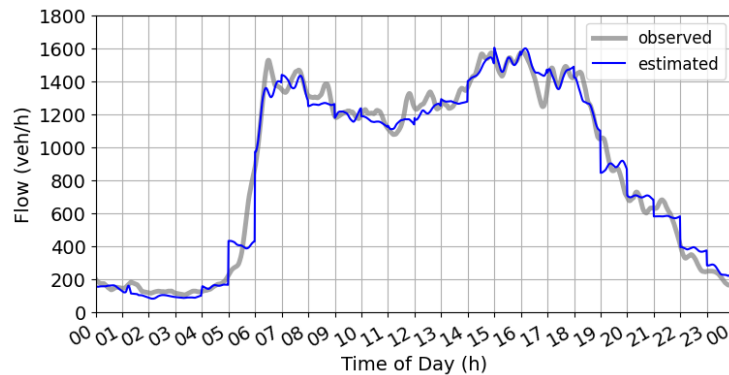
segments. We will also discuss travel time as an additional input feature for flow estimation in the following section.

Incorporating temporal factors into flow estimation improves the performance considerably. As shown in the table 5.2, the temporal ANN, which uses speed and time-related features, i.e., hour and day, as its independent variables, dramatically improves 88.3% on the south segment and 88.7% on the north segment over the baseline's performance. The temporal ANN's errors are nearly one-tenth of that in the baseline model for both segments (south MAPE = 11.54%, north MAPE = 14.40%). The result validates our hypothesis that incorporating temporal dependency into flow estimation provides more information to the ANN and better captures the dynamic flow-speed relationship that changes over time. The temporal ANN with travel time as its additional information source also shows a slight improvement over the temporal ANN without using the travel time, which is similar to the static ANN models. Notice that the performance differences between two adjacent road segments still exist when using temporal ANNs for estimation, but they are much smaller than those in the static ANN models.

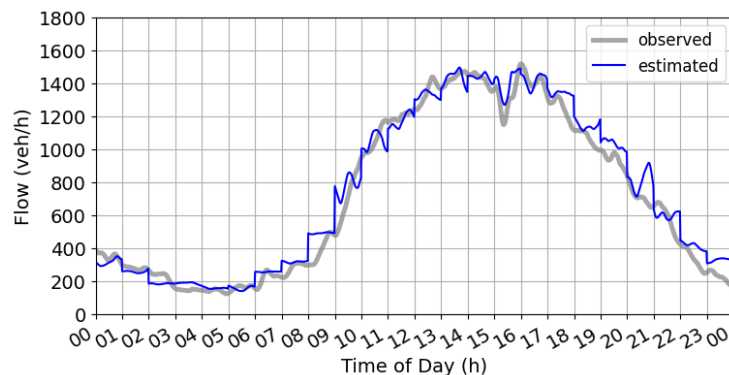
Finally, the spatiotemporal ANN, which incorporates time-related features, a space-related feature, and speed into flow estimation, achieves the best performance among all ANN models: a MAPE of 10.05% on the south and a MAPE of 10.75% on the north segment. It improves 89.8% over the baseline model on the south and 91.5% on the north. Spatiotemporal ANN not only has a negligible performance gap between the two road segments as we expected, but it also achieves a noticeable improvement on the south segment compared with the prior model scheme, i.e., temporal ANN (speed). Notice that the spatiotemporal ANN is the only model trained on the data from both road segments. We will discuss the spatial dependency and the benefits of using a spatiotemporal ANN in detail later.

Table 5.3 represents the overall estimation performance evaluated in RMSE for all models and the improvements achieved by ANN models compared with the baseline model. Although the values of improvements are different from the ones in MAPE, the overall trends of performance changes in RMSE are generally the same as the trends in MAPE regarding the changes made to the estimation model. However, one thing worth notice is that adding an additional source of traffic information, i.e., the travel time, into ANN models does not constantly improve the ANN's estimation performance in RMSE on the north segment. It could slightly degrade the ANN's performance on the north segment compared with the ANN without using the travel time. For example, in table 5.3, the ANN using both speed and travel time as independent

variables only achieves 6.0% improvement of RMSE on the north segment, which exhibits a decrement of 1.5% compared with the ANN using speed as its sole information source.



(a) Curves of estimated and observed flow on a weekday (22nd, Monday).

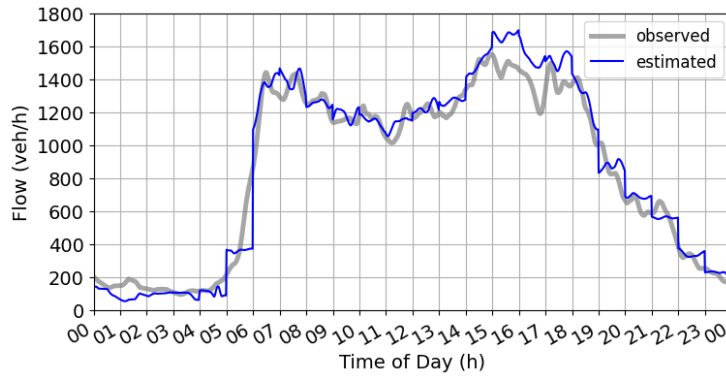


(b) Curves of estimated and observed flow in a weekend (28nd, Sunday).

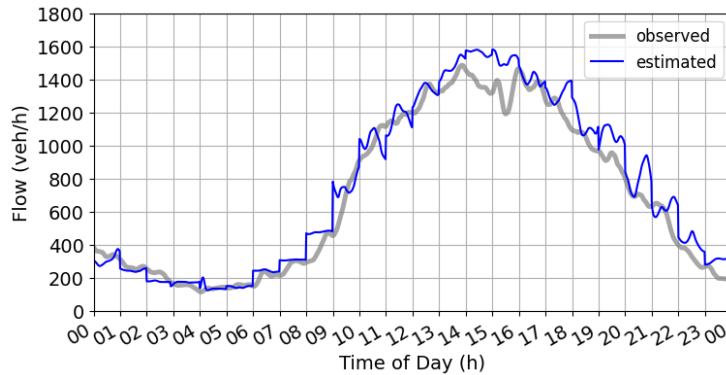
Figure 5.8 – Examples of estimated flows using temporal ANN (speed, travel time) on the south segment.

Figure 5.8 presents the estimated flows using the temporal ANN (speed, travel time) and the observed flows from the test dataset on the south segment. As shown in the figure, the ANN's estimated flows are pretty consistent with the fixed sensor's flows both on a weekday and a non-weekday. The model successfully captures the two-peak pattern on a typical weekday and the one-peak pattern on a non-weekday.

On the other hand, figure 5.9 shows the examples of the estimated flows and observed flows on the north road segment using the same temporal ANN. It is noticed that the model also works well most of the time on the north segment



(a) Curves of estimated and observed flow on a weekday (22nd, Monday).



(b) Curves of estimated and observed flow in a weekend (28th, Sunday).

Figure 5.9 – Examples of estimated flows using temporal ANN (speed, travel time) on the north segment.

but tends to overestimate the traffic flow when the flow is near capacity. The deviation of the estimated flows from the observed flows near capacity is because of some difference in traffic flow characteristics between the two road segments. Although the two road segments are very close to each other and have similar traffic flow relationships, the north segment's capacity is slightly lower than the south segment's. The temporal ANN, which was trained using the data solely from the south segment, always estimates the north segment's flow based on the south segment's capacity. Thus, deviations of estimation flows were observed near the capacity on the north segment.

Besides, we can observe that the curves of estimated flows are discontinuous at the transitions between hours because temporal ANN learned different traffic flow relationships to reflect the prevailing traffic condition in each hour.

As we discussed in section 5.2, using hours as thresholds to separate the traffic conditions is not a perfect method because traffic conditions are continuous rather than discrete and only change between hours. Moreover, incorporating hour segmentation as an explanatory variable into flow estimation may discretize the estimated values, especially when the traffic state changes sharply, for example, during the beginning of morning rush hours between 5 to 6 a.m. Nevertheless, as we demonstrated in this section, incorporating time of day and weekday as information into flow estimation is a practical method to improve the estimation accuracy on a road where the traffic conditions less change. Some more sophisticated time series methods in deep learning, e.g., LSTM, might solve the problems above when considering the temporal correlations between traffic states. It will be discussed as future works in the last chapter.

Generally speaking, using the new ML technique, i.e., ANN, and incorporating additional dependencies or information sources, i.e., temporal dependency, spatial dependency, and travel time, into flow estimation improves the performance compared with the classic flow-speed relationship model. As we exhibited that improvements in MAPE can be as significant as 89.8% on the south segment and 91.5% on the north. The best performer, i.e., spatiotemporal ANN, improves 293 veh/h in RMSE (76.8%) when used for traffic flow estimation on the south segment and 335 veh/h (79.3%) on the north segment over the baseline model. ANN models generally achieve more improvements on the north segment than on the south segment. However, notice that travel time as an additional information source contributes only tiny improvements and could cause slight performance degradation on the north segment when evaluated using RMSE, which should be utilized with extra care.

Chapter 6

Discussion

This chapter analyzes and discusses some phenomena we observed in the results from the previous section. First of all, we will discuss why the ANN produces a better estimation performance on the adjacent road segment than the classic flow-speed relationship. Then we will discuss the role the travel time plays as an additional information source for flow estimation, e.g., why its benefit to the performance improvement is weak? Finally, we will shortly discuss what might happen when we incorporate spatial dependency into our ANN model and use data from multiple road segments for training. We also discuss what benefits it could bring us if we train a central estimation model that learns spatial dependency for the entire road network with many road segments.

6.1 Input Speed Drift

In the flow estimation results, the ANN using speed as the independent variable improves more performance, i.e., larger than 10%, on the north segment than on the south segment. The result implies that the ANN model's performance degradation on the adjacent road segment is less severe than the baseline model's degradation. If a model can perform well on the road segments from which it has never seen data during the model training, we say it has good generality. Good generality of an estimation model is preferable because one of our goals is to use the model to estimate unobserved traffic flow on the road segments near the one where the model was trained.

However, why ANN model can perform more consistently on both road segments than the baseline model? We believe it is because ANN was trained on the scaled traffic variables rather than on traffic variables' original values.

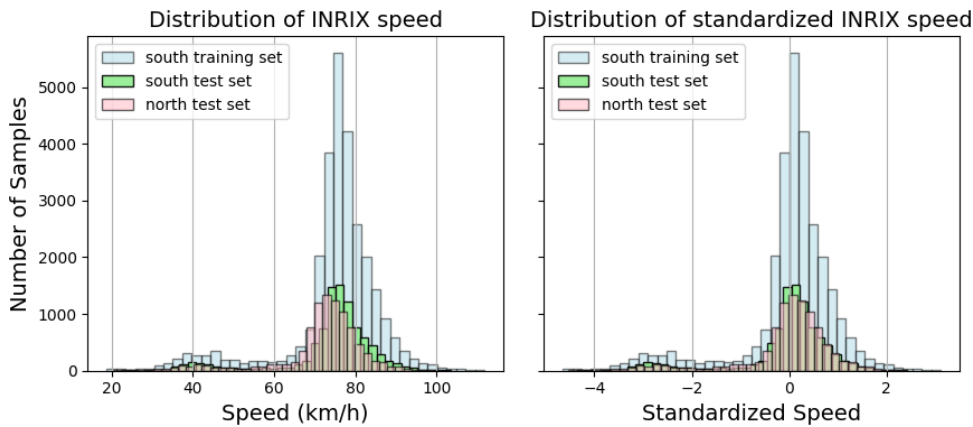


Figure 6.1 – Distributions of input speed in the training and test datasets before and after the standardization for the ANN (speed) model.

Remember the results of data preparation from the figure 5.3, the median speeds on the north segment are slower than the south segment. Figure 6.1 shows the speed distributions before and after the standardization in the training and test datasets for the baseline and ANN (speed) model. We can see that the distribution of speed on the north segment slightly drifts towards the left under the free-flow regime. Many reasons could cause the drift of free-flow speed between different road segments, e.g., varying speed limits on different links [6].

One reason for the baseline model's more severe performance degradation on the north segment is that we directly feed the north segment's speed into the flow-speed relationship as the evidence speed during the flow estimation. Notice that the flow-speed relationship in the baseline model was calibrated based on the south segment's speeds. The difference in speed distribution between two road segments could lead to the mismatch between the baseline flow-speed relationship and the flow-speed relationship lying in the samples observed on the north segment.

Figure 6.2 shows the test data from both segments and the flow estimations produced by the baseline model based on the corresponding speeds. As shown in the figure, the baseline model uses the same flow-speed relationship, which was calibrated using the training speed from the south, to estimate the flow on both segments. However, since the flow-speed relationship lying in the north segment's test samples, which are brown circles, drifts to the left compared with the south segment's flow-speed relationship, the baseline relationship does not suit the actual relationship on the north segment as on the south

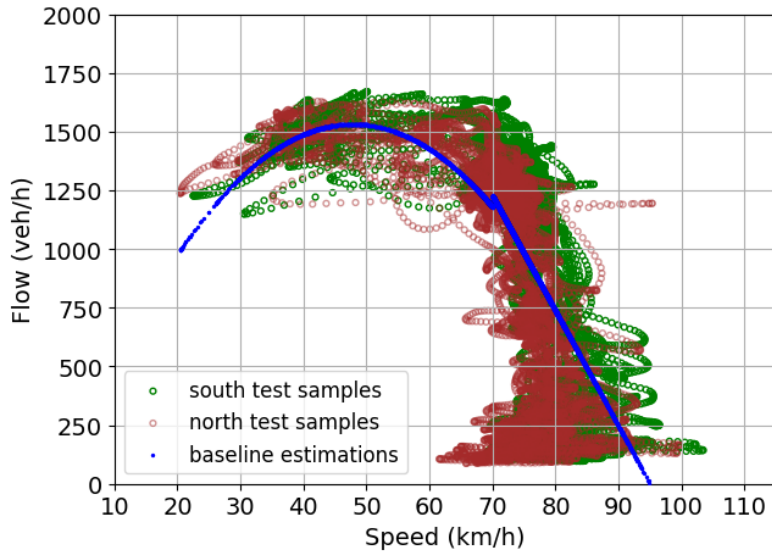
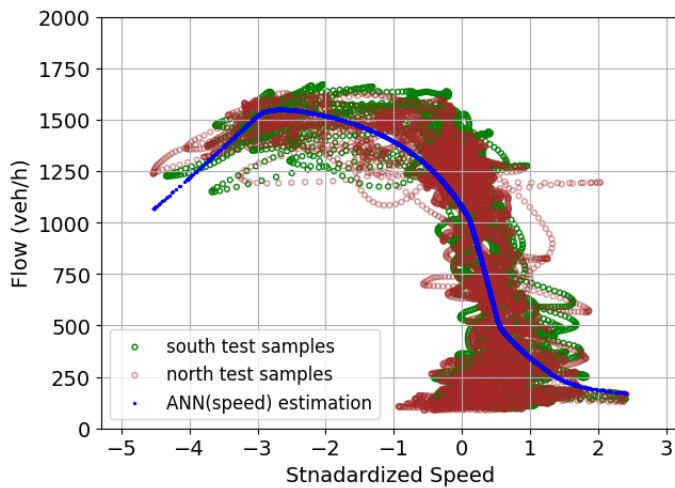


Figure 6.2 – Test samples from both road segments and corresponding flow estimations given by the baseline model.

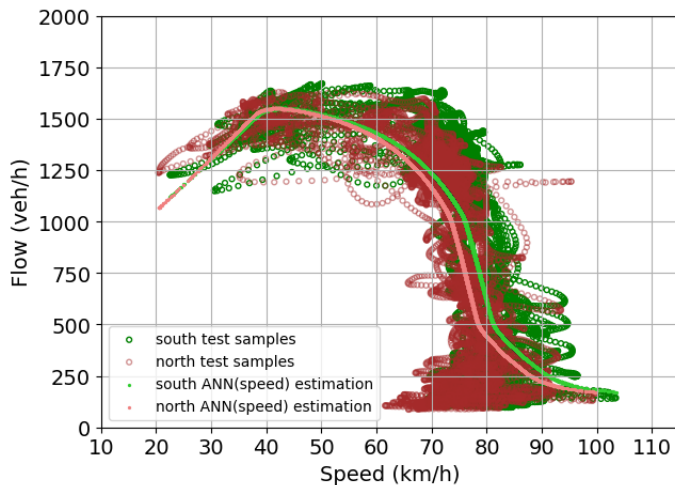
segment. The baseline, therefore, suffers from a more noticeable performance degradation on the north segment.

On the other hand, the ANN model was trained on the south road segment's standardized speed. As mentioned before, we standardized the test datasets' speeds by subtracting the historical mean value, which was obtained from the training dataset on the same road segment, from the original speed values, then dividing the values by the historical standard deviation. As shown in the figure 6.1, the distribution of standardized speeds on the north segment becomes similar to the south segment's speed distributions. The speed drift under the free-flow regime is disappeared. Figure 6.3a shows the test samples from both segments and the corresponding flow estimations produced by the ANN model, all based on the standardized speeds. We can see that the relationships between flow and standardized speed on the neighboring road segments are similar. The ANN relationship trained on the south segment's standardized speed could also fit the relationship between flow and standardized speed on its adjacent road segments.

Figure 6.3b shows the test samples on the two road segments and corresponding ANN model's estimations based on the actual speeds. The ANN model seems to adapt to the speed drift under the free-flow regime and split into two flow-speed relationships to fit each segment's samples. In conclusion, standardization of features gives ANNs better resistance to speed differences



(a) Flow-speed diagram based on the standardized speed.



(b) Flow-speed diagram based on the original speed.

Figure 6.3 – Test samples from both road segments and the corresponding flow estimations given by the ANN (speed) model.

between adjacent road segments. Although the ANN model is still far from a fully general model, it has better generality on neighboring road segments than the traditional flow-speed relationship.

6.2 Travel Time

As mentioned before, INRIX data, which is a kind of mobile data collected from probe vehicles, calculate the speed as the average speed of vehicles over

a length of the road, which is called space mean speed [17, 43]. Space mean speed can be calculated as following equation [14]:

$$v_{avg} = \frac{d}{\frac{1}{n} \sum_1^n t_i} \quad (6.1)$$

d = the distance over which travel times were measured

t_i = the travel time measured for the i^{th} vehicle

The denominator in equation 6.1 is the average travel time that vehicles take to travel across the road segment reported by the INRIX platform. Therefore, according to the equation, the INRIX speed and travel time are only two variables inversely proportional to each other. Figure 6.4 shows the relationship between speed and travel time in the south segment's training dataset. Although there are some variations in the data, we can see that the relationship between speed and travel time is indeed an inverse proportion. Based on this fact, we did not expect that the travel time would provide additional helpful information than the speed in flow estimation.

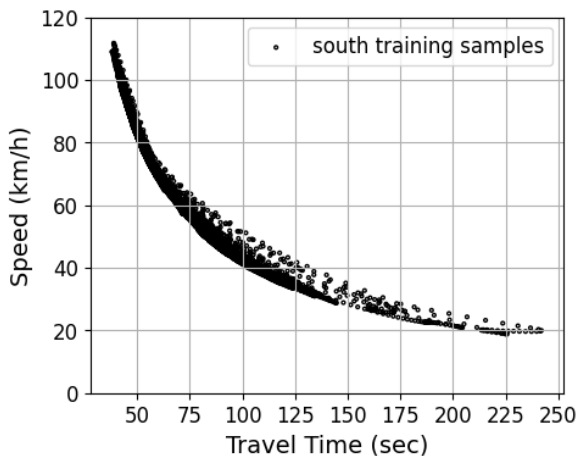


Figure 6.4 – Relationship between speed and travel time in the training dataset from the south road segment.

However, adding travel time still improves the estimation performance slightly, as we demonstrated in section 5.3. One possible reason is that travel time as an additional feature may complement speed when the speed value is small. As shown in figure 6.4, when the speed is small, e.g., below 40 km/h, the speed changes are also small. On the other hand, changes in travel times

under this regime are more pronounced, providing additional information for the model to recognize different traffic states and flows. Nevertheless, the improvement that travel time could bring is slight compared to other techniques such as temporal dependency.

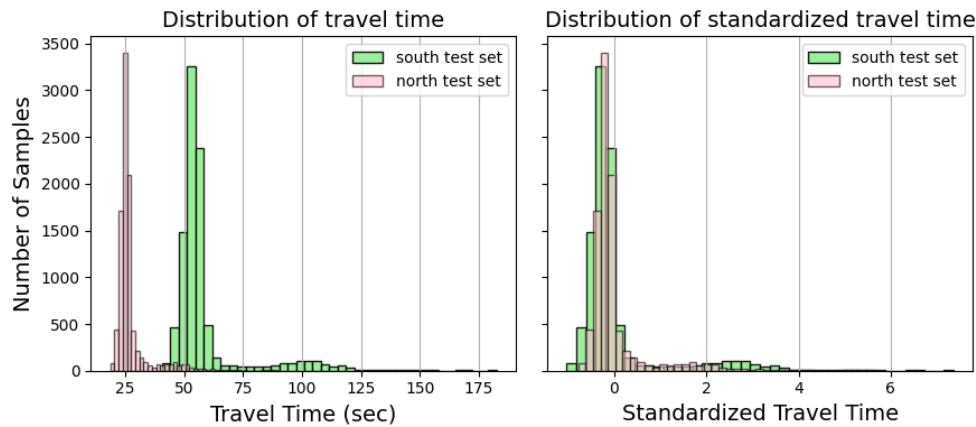


Figure 6.5 – Distributions of travel time in the test datasets before and after the standardization.

As we demonstrated in the result of flow estimation, travel time could sometimes worsen the model's performance on the adjacent road segment instead of improving it. After examining the datasets on the north segment between 1st and 21nd October, we found some severe congestions occurred on the north segment but not south. The severe congestions resulted in some high travel times, which could be as large as ten times the median travel time. The high values affect travel time's distribution on the north segment, leading to the different distributions between two road segments after the standardization. Because our ANN (speed, travel time) model was trained based on the standardized travel times from the south segment without experiencing severe congestions, there will be a slight mismatch between the trained ANN relationship and the north's relationship. This mismatch causes the performance deterioration on the north segment, similar to the baseline model case. The difference is that this time the standardization cannot eliminate the fundamental difference in travel time distribution between two road segments caused by the congestions. Figure 6.5 shows the distributions of travel times in both segments' test datasets before and after the standardization. As shown in the figure, the difference in travel time distribution between two road segments, i.e., the different standard deviations, still exists after the standardization.

In contrast, speed as an information source for estimation is less affected by congestions. Theoretically, while the travel time could increase fast and unlimitedly as the congestion piles up, the speed changes relatively little and has a minimum value of 0 km/h. Therefore, the speed distribution is less affected by the congestions, and the standardized speeds are similar on the adjacent road segment, as shown in figure 6.1. In conclusion, the speed is a better choice of information source for flow estimation than the travel time because the traffic flow relationship trained on the standardized speeds is less affected by the variations in traffic conditions, and it consistently fits the samples on different road segments.

6.3 Spatial Dependency

As we demonstrated in the flow estimation results, when we incorporated the spatial dependency into flow estimation, the performance gaps observed in all other estimation models between the south and north segments disappear. Because we trained the spatiotemporal ANN using data from both road segments and adopted a location feature for identifying each segment, the model could learn the unique characteristics of the time-varying traffic flow relationship on the north segment, just like it did on the south. Thus the spatiotemporal ANN achieves a consistent performance on both segments.

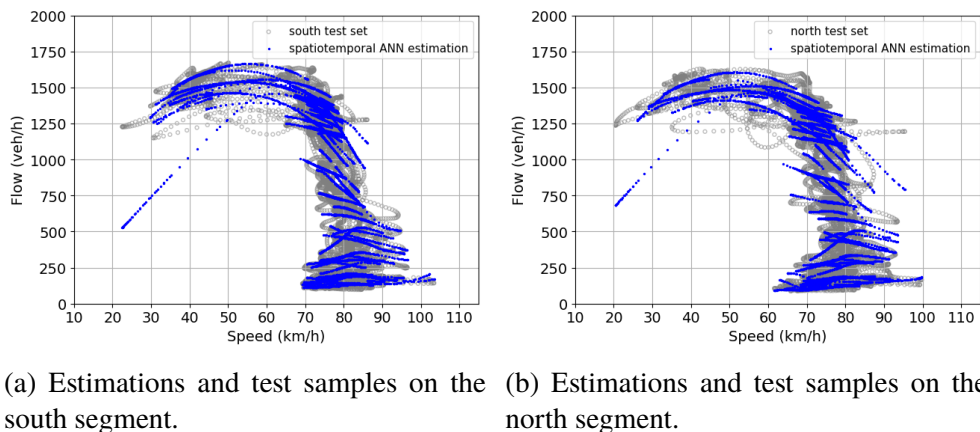


Figure 6.6 – Spatiotemporal ANN’s flow estimations on both road segments.

However, to our surprise, considering the spatial dependency not only improves the performance on the adjacent road segment but also achieves a noticeable improvement on the south segment compared with the temporal ANN. For example, as shown in table MAPE and table RMSE, the spatiotemporal

ANN achieves 1.6% more improvement in MAPE and 2.2% more improvements in RMSE on the south segment relative to the temporal ANN (speed), which does consider the spatial dependency. Our explanation for this improvement on the south segment is that the exploitation of data from multiple road segments may provide the ANN model with more traffic data patterns. That additional information helps the ANN learn a more comprehensive and universal flow-speed relationship and better estimate the traffic flows on the south segment than the model trained on data from only one segment. One indirect evidence for the explanation could be found in figure 6.6, which presents the spatiotemporal ANN's flow estimations and the test samples for both segments. Although there are deformation and position differences between the two estimations in the flow-speed diagrams, e.g., the relationship curve's height is smaller on the north segment than on the south. We can see that the time-varying flow-speed relationships given by the spatiotemporal ANN on both segments are very similar. Considering there are only 120 parameters corresponding to the model's location feature, the model cannot learn an entirely new time-varying relationship for each segment. Spatiotemporal ANN more likely learned a universal time-varying flow-speed relationship shared by both segments and captured each segment's relationship's unique characteristics according to their location feature, e.g., shorten the height of the relationship curve for the north segment. Thus more training data improves the universal relationship shared by both segments and further improves the model's performance on the south segment. Unfortunately, it is not easy to analyze how spatiotemporal ANN works internally and prove our explanation's correctness since the ANN is a black-box model.

We can, of course, build and train many small ANN models for estimating flows on road segments in a network instead of building an ANN considering spatial dependency. However, spatiotemporal ANN shows the possibility of a central estimation model that learns the spatiotemporal dependencies for the entire road network and might provide some benefits over single segment models. First, it could reduce the number of estimation models needed by ITS for estimating the traffic flow in a road network. A central estimation model will have fewer parameters than the combination of many small models, a more efficient way to model the traffic dynamics in a transportation system with many road segments. Second, as we discussed above, training a model using data from multiple road segments might improve the overall performance on every road segment covered by the model compared with using data from a single road segment for training. Because the central estimation model is more complex than the single segment model, it might also suffer from long training

and computational time. However, we need to validate spatiotemporal ANN's performance and benefits when building a central estimation model on a road network with many road segments via network-wide sensor data.

6.4 Model Usage and updates

Finally, we shortly discuss the use of ANN models proposed in this work for flow estimation/imputation and the update of models over time.

The situation is simple when we use the ANN models to impute the missing data due to fixed sensor malfunctions or communication failures on the road segments. We use the ANN model trained on the historical data, i.e., data in the training set, to impute the missing flow data on the same road segment where the model was trained. The case is similar to what we did when using the ANN models trained on E4's south road segment to estimate the traffic flow on the same segment between 22nd and 28th October.

However, when we intend to use the models for estimating the traffic flow on the road segments and regions where there is no fixed sensor installed and the traffic flow is never observed, the situation is more complex than the imputation. We knew that the training of a model strongly depends on many factors, e.g., number of lanes, speed limit, road surface, road's geometric alignment, road type, and much more [2, 6], all of which may affect the traffic flow characteristics on a road, e.g., capacity and free-flow speed. Thus, a model trained on one road segment may not be suitable for another road segment with different traffic flow characteristics. Using an inappropriate model for estimation will lead to erroneous results.

When our goal is to estimate the traffic flow on the road segments between two adjacent fixed sensors, as shown in figure 2.1, the situation is relatively simple. We assume that a segment's traffic characteristics do not change much from the nearest sensor locations because the usual space between sensors is only several hundred meters to few kilometers. Based on the assumption, we have two alternative approaches to choose the model for estimating the flow on the road segment. The first approach is choosing the ANN model trained on the physically nearest road segment with the fixed sensor installed. For example, in this project, we estimated the flow on E4's north road segment using temporal ANN models trained on its nearest road segment with a fixed sensor, i.e., the south segment in the distance of 1 km. As we demonstrated, the models produced satisfied estimation results on the north segment, whose performance is only slightly worse than that on the south segment. Note that in the case of using spatiotemporal ANN, we assign the nearest fixed sensor's

location feature to the evidence data samples on the target segment to select the traffic flow relationship to be used.

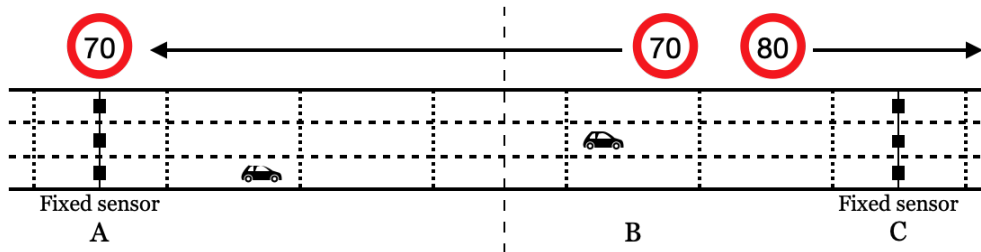


Figure 6.7 – Conceptual representation for a road segment between two fixed sensors with a speed limit transition.

However, the first approach could lead to a problem that the nearest segment might not have the most similar traffic flow characteristics as the target road segment. Figure estimation shows an example for this problem. In figure estimation, road segment B between fixed sensor segment A and C is the target segment for estimating the flow. Although B is closer to the C segment, B's speed limit is the same as A's speed limit. As we discussed in the previous sections, different speed limits and probably other factors might cause different speed distributions, resulting in different traffic flow characteristics on different road segments. Therefore, using the C segment estimation model, which has the nearest fixed sensor and a speed limit of 80 km/h, might not be a better choice than choosing the A segment's model in this case. To solve this problem, we propose a second approach is to choose the estimation model from the road segment that has a similar speed distribution, i.e., standard deviation and mean speed, as the target road segment out of the nearest two segments with fixed sensors.

On the other hand, if we want to use the trained models to estimate the flows for road segments on different roads in a road network or on the same roads but far from where the models were trained, the problem will be much more complicated. The traffic flow characteristics on those target road segments could be very different from the segments where the models trained. We could adopt an approach proposed by Neumann et al. [6] for this use case. According to Neumann, first, we need to identify a scheme of factors, e.g., number of lanes, speed limit, road type, that affect the traffic flow characteristics. Based on the scheme, we group all roads into several classes. The roads within a class have similar traffic characteristics. Finally, we train an estimation model on one road segment for each class and estimate the flow on the same class's road segments using this model. By adopting this approach, estimation models'

usage will not be confined to the regions in proximity to fixed sensors anymore. Moreover, we could use it in a geographically broader region in a road network. However, identifying the factors that affect traffic flow characteristics and developing a practical scheme for classifying homogenous road classes is difficult. It is hence out of this thesis's scope. Nevertheless, ANN's ability to learn complex relationships in the high dimensional dataset, as we have shown in this work, still makes it a competitive candidate when building a more general model that incorporates all influential factors into flow estimation in a road network.

Finally, we need to regularly update and retrain our estimation models using the new observed dataset once deployed in ITS. As a common phenomenon in machine learning, almost all the models degrade over time, so do our estimation models. For example, the ANN model trained before the lockdown will probably perform poorly once the government implements a lockdown due to the 2020 pandemic. The driver's behavior in rush hours will be very different when people start to work from home. Therefore, regularly monitor the model and retrain it with the newly updated datasets is very important to ensure that the model can learn the new traffic flow characteristics and its performance does not drop. Fortunately, automating the processes of building and training the machine learning models we proposed is very simple because our approach is highly automated. One only needs to regularly run the script we provided in the Github repository to build and train the estimation models, for example, every week using updated data via some common scheduling commands in Unix.

Chapter 7

Conclusion and Future work

This thesis proposed a new approach to estimate or impute the traffic flow on highways based on a machine learning method, i.e., feed-forward ANN, and an alternative data source, i.e., INRIX mobile data. The basic idea is using ANN model to extract the relationships between fixed radar sensor's traffic flow and INRIX mobile data's measures in different time periods on a road segment from the historical data, and then using real-time INRIX data as model's inputs to inference the traffic flow in the periods and neighboring regions when and where the flow data is not observed.

We first developed a set of data-preparation processes to prepare the raw data for training the ANNs. The data-preparation methods included filtering the low-quality data in the datasets, smoothing noises via moving average, removing the measurement latency by shifting data's timestamps, scaling the input features, and preparing one-hot encoding features denoting the temporal and spatial factors. We implemented and tested several ANN models to capture the traffic flow relationships while considering temporal and spatial dependencies and an additional INRIX measure, i.e., travel time. The results showed that ANN models could capture the traffic conditions that vary depending on the time period of a day, the day of a week, and the road segments' location to a certain level. Generally speaking, the models' estimation performance improved when we incorporated a new dependency or explanatory variable as an input feature.

Compared with a multi-regime regression baseline model representing the typical stationary flow-speed relationship, all ANN models outperformed the baseline model. We also found that the ANN models exhibited more consistent performance on the adjacent road segment than the baseline model, which implied that ANN is a more promising candidate for estimating the traffic

flow in the nearby region of a fixed sensor. However, we found that the incorporation of travel time as an additional input feature might slightly worsen the model's estimation accuracy on the neighboring road segment. Therefore, we suggested using travel time as ANN models' input feature with extra care when the models might be used for estimating the traffic flow on a different road segment near the fixed sensor. We also provided some possible reasons for the above results and the characteristics observed in our approach.

Although the ANN-based approach proposed in this work might provide little insights into traffic flow theory, it is an efficient method to estimate or impute the traffic flow with reasonable accuracy using mobile data in a border spatial and temporal region. Moreover, it provides a highly automated means to process sensor data and build estimation models for ITS effortlessly in a road network having many road segments and large-scale sensor data. As a result, the proposed approach should benefit various ITS applications.

7.1 Future work

In this section, we discuss some possible directions for future researches as an extension of this thesis.

7.1.1 Spatial-Temporal Correlations

Mining spatial and temporal information in the spatial-temporal correlation datasets is a prevalent topic in traffic data imputation and prediction. Like we mentioned in the delimitation of the thesis in Chapter 1, we did not use the temporal and spatial correlation between neighboring data points in the time-space domain for traffic flow estimation and imputation. We did capture the traffic condition's dependency on the hour/weekday and location in the historical data and used this information to inference the traffic flow based on the real-time INRIX measures. However, more information is hidden in an unobserved/missing data point's neighboring data in the time-space domain. For example, a road segment's traffic flow could be heavily affected by the traffic conditions from its upstream and downstream road segments.

Moreover, traffic flow in a time slice could have strong correlations with traffic conditions in its previous and later few time slices. Therefore, full use of spatial-temporal information could help us improve the accuracy of traffic flow estimation, imputation, or prediction. One possible direction for future research is to collect a comprehensive dataset containing INRIX and MCS data collected from many road segments on the road or in a road network during an

extended period. Then, one could use sophisticated deep learning methods such as [Recurrent Neural Network \(RNN\)](#), [CNN](#), or [Graph Convolutional Network \(GCN\)](#) to extract the temporal and spatial correlations between traffic flow and INRIX's measures from the dataset containing rich spatial-temporal information. The extracted spatial-temporal correlations and real-time INRIX measures could be solely used for estimating the traffic flow on a road segment, like what we did in this work, or could be used together with other fixed sensor data for estimating, imputing, or predicting the traffic flow.

7.1.2 Traffic Flow Prediction

Predicting short-term traffic flow is a challenging but more valuable task for traffic control ITS and transportation planning. Therefore, one possible future direction is extending the approach proposed in this thesis to work for traffic flow forecasting. Most studies use features solely from the fixed-location sensor's measures to predict traffic flow to the best of the author's knowledge. At the same time, very few of them took alternative data sources, e.g., mobile data, into account when it comes to traffic prediction. The quickest way to extend our approach for traffic forecasting is using flows in the short-term future, e.g., 15 minutes, as labels to train our ANN models, and then using the models to predict the traffic flow based on the current INRIX measures.

However, a typical prediction approach will be extracting the temporal correlations from the historical data using some time-series models, e.g., RNN or [Long Short-Term Memory \(LSTM\)](#), and then using the extracted correlation for prediction based on the recent INRIX data from the current and previous time slices. Some recent studies also captured the spatial correlation and the temporal correlation using GCN to make full use of both spatial and temporal information in a road network for traffic forecasting [44]. No matter which method one uses to extract the temporal and/or spatial correlations between INRIX measures and the traffic flow, INRIX data as an additional information source should help improve the prediction accuracy when used together with the typical fixed sensor's measures. Besides, we could also use INRIX alone for predicting the short-term traffic flow when other data sources are not available, e.g., the fixed detector malfunctions.

7.1.3 Others

One could make other improvements in future studies. In the data preparation part of this work, we removed INRIX speed's time-lag by shifting its time-

series curve by a time slice and examined if it overlapped with MCS's curve iteratively until the two curves were overlapped. In the future, one could use Fourier analysis to decide the value of timestamps to be shifted to ensure two time-series curves overlap with each other accurately. Finally, as we mentioned, traffic conditions and traffic flow relationships are influenced by many factors, e.g., number of lanes, weather, special event, road surface, road's geometric alignment, and much more. In future works, one could consider more influencing factors and more data sources, e.g., extended floating car data, to improve the model's estimation accuracy. Moreover, one might develop a genuinely general model that can estimate traffic flow on all road segments in a road network by incorporating most of the essential influencing factors into the estimation.

References

- [1] M. Barth and K. Boriboonsomsin, “Real-world co2 impacts of traffic congestion,” in *PREPARED FOR THE 87TH ANNUAL MEETING OF THE TRANSPORTATION RESEARCH BOARD*. Citeseer, 2007.
- [2] T. Seo, A. M. Bayen, T. Kusakabe, and Y. Asakura, “Traffic state estimation on highway: A comprehensive survey,” *Annual reviews in control*, vol. 43, pp. 128–151, 2017.
- [3] N. Tsanakas, *Emission estimation based on traffic models and measurements*. Linköping University Electronic Press, 2019, vol. 1835. ISBN 9176850927
- [4] Y. Duan, Y. Lv, Y.-L. Liu, and F.-Y. Wang, “An efficient realization of deep learning for traffic data imputation,” *Transportation research part C: emerging technologies*, vol. 72, pp. 168–181, 2016.
- [5] K. Anuar, F. Habtemichael, and M. Cetin, “Estimating traffic flow rate on freeways from probe vehicle data and fundamental diagram,” in *2015 IEEE 18th International Conference on Intelligent Transportation Systems*. IEEE, 2015, Conference Proceedings. ISBN 1467365963 pp. 2921–2926.
- [6] T. Neumann, P. L. Böhnke, and L. C. T. Tcheumadjeu, “Dynamic representation of the fundamental diagram via bayesian networks for estimating traffic flows from probe vehicle data,” in *16th International IEEE Conference on Intelligent Transportation Systems (ITSC 2013)*. IEEE, 2013, Conference Proceedings. ISBN 147992914X pp. 1870–1875.
- [7] S. Blandin, A. Salam, and A. Bayen, “Individual speed variance in traffic flow: analysis of bay area radar measurements,” in *Transportation Research Board 91st Annual Meeting*, 2012, Conference Proceedings.

- [8] E. Bulteau, R. Leblanc, S. Blandin, and A. Bayen, “Traffic flow estimation using higher-order speed statistics,” in *Transportation Research Board 92nd Annual Meeting*, 2013, Conference Proceedings.
- [9] E. Parliament, “Directive 2010/40/eu of the european parliament and of the council of 7 july 2010 on the framework for the deployment of intelligent transport systems in the field of road transport and for interfaces with other modes of transport,” *Off. J. Eur. Union*, pp. 1–13, 2010.
- [10] A. Sumalee and H. W. Ho, “Smarter and more connected: Future intelligent transportation system,” *IATSS Research*, vol. 42, no. 2, pp. 67–71, 2018.
- [11] X. Ma, Z. Tao, Y. Wang, H. Yu, and Y. Wang, “Long short-term memory neural network for traffic speed prediction using remote microwave sensor data,” *Transportation Research Part C: Emerging Technologies*, vol. 54, pp. 187–197, 2015.
- [12] E. I. Vlahogianni, J. C. Golias, and M. G. Karlaftis, “Short-term traffic forecasting: Overview of objectives and methods,” *Transport reviews*, vol. 24, no. 5, pp. 533–557, 2004.
- [13] A. Håkansson, “Portal of research methods and methodologies for research projects and degree projects,” in *The 2013 World Congress in Computer Science, Computer Engineering, and Applied Computing WORLDCOMP 2013; Las Vegas, Nevada, USA, 22-25 July*. CSREA Press USA, 2013, Conference Proceedings, pp. 67–73.
- [14] L. Elefteriadou, *An introduction to traffic flow theory*. Springer, 2014, vol. 84.
- [15] C. Chen, J. Kwon, J. Rice, A. Skabardonis, and P. Varaiya, “Detecting errors and imputing missing data for single-loop surveillance systems,” *Transportation Research Record*, vol. 1855, no. 1, pp. 160–167, 2003.
- [16] J. C. Herrera, D. B. Work, R. Herring, X. J. Ban, Q. Jacobson, and A. M. Bayen, “Evaluation of traffic data obtained via gps-enabled mobile phones: The mobile century field experiment,” *Transportation Research Part C: Emerging Technologies*, vol. 18, no. 4, pp. 568–583, 2010.

- [17] A. Sharma, V. Ahsani, and S. Rawat, “Evaluation of opportunities and challenges of using inrix data for real-time performance monitoring and historical trend assessment,” *Reports and White Papers*, vol. 24, 2017.
- [18] S. Kim and B. Coifman, “Comparing inrix speed data against concurrent loop detector stations over several months,” *Transportation Research Part C: Emerging Technologies*, vol. 49, pp. 59–72, 2014.
- [19] T. Seo, T. Kusakabe, and Y. Asakura, “Traffic state estimation with the advanced probe vehicles using data assimilation,” in *2015 IEEE 18th International Conference on Intelligent Transportation Systems*. IEEE, 2015, Conference Proceedings. ISBN 1467365963 pp. 824–830.
- [20] J. Van Lint and C. Van Hinsbergen, “Short-term traffic and travel time prediction models,” *Artificial Intelligence Applications to Critical Transportation Issues*, vol. 22, no. 1, pp. 22–41, 2012.
- [21] S. P. Hoogendoorn and V. Knoop, “Traffic flow theory and simulation,” 2016, accessed: 2020-11-03. [Online]. Available: <https://ocw.tudelft.nl/courses/traffic-flow-theory-simulation/>
- [22] G. Dervisoglu, G. Gomes, J. Kwon, R. Horowitz, and P. Varaiya, “Automatic calibration of the fundamental diagram and empirical observations on capacity,” in *Transportation Research Board 88th Annual Meeting*, vol. 15. Citeseer, 2009, pp. 31–59.
- [23] T. Seo, Y. Kawasaki, T. Kusakabe, and Y. Asakura, “Fundamental diagram estimation by using trajectories of probe vehicles,” *Transportation Research Part B: Methodological*, vol. 122, pp. 40–56, 2019.
- [24] G. F. Newell, “A simplified theory of kinematic waves in highway traffic, part i: General theory,” *Transportation Research Part B: Methodological*, vol. 27, no. 4, pp. 281–287, 1993.
- [25] L. Immers and S. Logghe, “Traffic flow theory,” *Faculty of Engineering, Department of Civil Engineering, Section Traffic and Infrastructure, Kasteelpark Arenberg*, vol. 40, p. 21, 2002.
- [26] H.-N. Nguyen, B. Fishbain, E. Bitar, D. Mahalel, and P.-O. Gutman, “Dynamic model for estimating the macroscopic fundamental diagram,” *IFAC-PapersOnLine*, vol. 49, no. 3, pp. 297–302, 2016.

- [27] C. Antoniou and H. N. Koutsopoulos, “Estimation of traffic dynamics models with machine-learning methods,” *Transportation research record*, vol. 1965, no. 1, pp. 103–111, 2006.
- [28] T. Neumann, L. C. Touko Tcheumadjeu, P. L. Böhnke, E. Brockfeld, and X. Bei, “Deriving traffic volumes from probe vehicle data using a fundamental diagram approach,” in *13th World Conference on Transport Research (WCTR)*, 2013.
- [29] Wikipedia contributors, “Linear regression — Wikipedia, the free encyclopedia,” 2021, [Online; accessed 11-February-2021]. [Online]. Available: https://en.wikipedia.org/w/index.php?title=Linear_regression&oldid=1005047010
- [30] A. Géron, *Hands-on machine learning with Scikit-Learn, Keras, and TensorFlow: Concepts, tools, and techniques to build intelligent systems*. O’Reilly Media, 2019. ISBN 1492032611
- [31] D. Nikovski, N. Nishiuma, Y. Goto, and H. Kumazawa, “Univariate short-term prediction of road travel times,” in *Proceedings. 2005 IEEE Intelligent Transportation Systems, 2005*. IEEE, 2005, pp. 1074–1079.
- [32] W. S. McCulloch and W. Pitts, “A logical calculus of the ideas immanent in nervous activity,” *The bulletin of mathematical biophysics*, vol. 5, no. 4, pp. 115–133, 1943.
- [33] F. Rosenblatt, *The perceptron, a perceiving and recognizing automaton Project Para*. Cornell Aeronautical Laboratory, 1957.
- [34] D. E. Rumelhart, G. E. Hinton, and R. J. Williams, “Learning internal representations by error propagation,” California Univ San Diego La Jolla Inst for Cognitive Science, Report, 1985.
- [35] M. R. Wilby, J. J. V. Díaz, A. B. Rodríguez González, and M. Á. Sotelo, “Lightweight occupancy estimation on freeways using extended floating car data,” *Journal of Intelligent Transportation Systems*, vol. 18, no. 2, pp. 149–163, 2014.
- [36] Y. Wang, M. Papageorgiou, A. Messmer, P. Coppola, A. Tzimitsi, and A. Nuzzolo, “An adaptive freeway traffic state estimator,” *Automatica*, vol. 45, no. 1, pp. 10–24, 2009.

- [37] Y. Zhuang, R. Ke, and Y. Wang, “Innovative method for traffic data imputation based on convolutional neural network,” *IET Intelligent Transport Systems*, vol. 13, no. 4, pp. 605–613, 2018.
- [38] M. Zhong, S. Sharma, and Z. Liu, “Assessing robustness of imputation models based on data from different jurisdictions: examples of alberta and saskatchewan, canada,” *Transportation research record*, vol. 1917, no. 1, pp. 116–126, 2005.
- [39] Z. Liu, S. Sharma, and S. Datla, “Imputation of missing traffic data during holiday periods,” *Transportation Planning and Technology*, vol. 31, no. 5, pp. 525–544, 2008.
- [40] D. Ni and J. D. Leonard, “Markov chain monte carlo multiple imputation using bayesian networks for incomplete intelligent transportation systems data,” *Transportation research record*, vol. 1935, no. 1, pp. 57–67, 2005.
- [41] O. A. Nielsen and R. M. Jørgensen, “Estimation of speed–flow and flow–density relations on the motorway network in the greater copenhagen region,” *IET Intelligent Transport Systems*, vol. 2, no. 2, pp. 120–131, 2008.
- [42] H.-T. Cheng, L. Koc, J. Harmsen, T. Shaked, T. Chandra, H. Aradhye, G. Anderson, G. Corrado, W. Chai, M. Ispir *et al.*, “Wide & deep learning for recommender systems,” in *Proceedings of the 1st workshop on deep learning for recommender systems*, 2016, pp. 7–10.
- [43] V. Ahsani, M. Amin-Naseri, S. Knickerbocker, and A. Sharma, “Quantitative analysis of probe data characteristics: Coverage, speed bias and congestion detection precision,” *Journal of Intelligent Transportation Systems*, vol. 23, no. 2, pp. 103–119, 2019.
- [44] T. Zhang, J. Jin, H. Yang, H. Guo, and X. Ma, “Link speed prediction for signalized urban traffic network using a hybrid deep learning approach,” in *2019 IEEE Intelligent Transportation Systems Conference (ITSC)*. IEEE, 2019, pp. 2195–2200.

For DIVA

```
{  
  "Author1": { "name": "Pei-Lun Hsu"},  
  "Degree": { "Educational program": ""},  
  "Title": {  
    "Main title": "ML-Based Data-Driven Traffic Flow Estimation from Mobile Data",  
    "Language": "eng" },  
    "Alternative title": {  
      "Main title": "ML-baserad datadriven uppskattning av trafikflöden från mobila data",  
      "Language": "swe"  
    },  
    "Supervisor1": { "name": "Ian Marsh, Xiaoliang Ma" },  
    "Examiner": {  
      "name": "Erik Jenelius",  
      "organisation": { "L1": "School of Electrical Engineering and Computer Science" }  
    },  
    "Cooperation": { "Partner_name": "RISE SICS AB"},  
    "Other information": {  
      "Year": "2021", "Number of pages": "xi,73"}  
}
```